

Self-assembly of Block Copolymers in Ionic Liquids

Ru Chen[†], Carlos R. López-Barrón[‡], Norman J. Wagner[†]

[†] Center for Neutron Science, Department of Chemical and Biomolecular Engineering, University of Delaware, Newark, Delaware 19716, United States

[‡] ExxonMobil Chemical Company, Baytown Technology and Engineering Complex, Baytown, Texas 77520, United States

*corresponding author: wagnernj@udel.edu

Abstract

Self-assembly of amphiphilic block copolymers can impart desired discrete or continuous nanostructures, such as micelles utilized as drug delivery vehicles in aqueous solvents, or cross-linked micelles for stretchable electronics fabrications in ionic liquids. These appealing applications have motivated significant research efforts to understand the nano- and microstructure as well as the structure-property relationships underlying such self-assembled systems, with the ultimate goal being effective formulation. To take full advantage of the bottom-up self-assembly approach, a comprehensive understanding of the factors that govern the self-assembly behavior of dilute, concentrated and functionalized system of non-ionic block copolymers self-assembly in ionic liquids, as well as robust characterization methods for quantifying the microstructure and properties relationship must be reviewed. For each system, the most significant challenges are presented and discussed. In addition, current and potential applications of block copolymers/ionic liquid system are also discussed. This provides a measure of the current state of understanding, which motivates a brief look forward towards future directions in this field.

Introduction

Well-defined nanostructured materials are of considerable interest due to their emergent properties that can be exploited in various applications.¹ As a result, the development of methodologies for their formulation and fabrication motivates research into their nanostructure and its relationship to the desired properties. One of the most universal techniques to prepare those materials with tunable and controllable morphologies is by self-assembly of amphiphilic block copolymers (ABCs) in selected self-assembly media. Self-assembled nanostructures in aqueous solutions have found applications in emerging nanotechnologies, including drug delivery vehicles and aqueous nanoreactors. However, self-assembly in ionic liquids (ILs) has been mainly utilized in material science for engineering novel, hierarchically structured solid or soft-solid materials in ion-conducting electrolytes or wearable electronics applications. In addition to those technological applications, ABC/IL systems also provide important fundamental scientific significance. Prior to the use of IL as a self-assembly media, ABC aqueous micellar solutions has been a commonly used model system for studying molecular interactions between non-ionic surfactants and molecular solvents, as well as thermodynamics and kinetics involved in the micellization process. Furthermore, with the addition of charged ions, ABC wormlike micellar nanocolloids create another model system for studying non-linear flow phenomena and flow instabilities such as shear banding. Using ILs as self-assembly media not only opens up a new line of investigation where self-assembly is not determined in part by Coulombic interactions, but also opens a new model paradigm for studying micellization and the associated physiochemical properties of microphase transitions. As will be demonstrated in this chapter, there has been a significant amount of recent research exploring the microstructure and possible emergent properties of self-assembled ABC/IL systems is warranted. Accordingly, this chapter provides an up-to-date literature review on the field of ABCs self-assembly in ILs, which identifies some key findings that should be of interest to practitioners and researchers alike working with block co-polymers and non-ionic surfactants in ILs. This chapter starts with a brief review on the differences and similarities between the self-assembly of ABCs in ILs versus water environment, which is followed by a detailed review on the self-

assembled microstructure-property relationship of representative ABC/IL micellar systems under static and flow conditions. We conclude with a brief discussion of emerging and potential applications as well as future directions in this field. For the purpose of this review, only non-ionic ABCs will be included. We do not seek to comprehensively survey all existing ABC/IL systems, but instead to provide some perspectives on the current understanding, characterization techniques, challenges and opportunities that could be realized to assist in better formulation and in the development of new applications. While space limitations restrict how much that can be included, we refer the reader to recent, relevant reviews of the structure of ILs,^{2,3} ILs as self-assembly media,^{4,5} polymers in ILs⁶ and IL polymer electrolytes.^{7,8}

Current understanding on self-assembly of amphiphilic block copolymers in ionic liquids versus other self-assembly media

In conventional material design, due to the limited amount of known self-assembly media,⁵ tailoring a self-assembly system to meet specific design properties often requires modifying the components, compositions and architecture of ABCs. This subject has been extensively reviewed¹ and is now a textbook topic.⁹⁻¹¹ With the identification of ILs to be capable of promoting ABCs self-assembly, the number of self-assembly systems has increased dramatically. Currently, one molecular solvent (water), three protic ILs (PILs, mainly with alkylammonium cations) and nine aprotic ILs (AILs, mainly with imidazolium cations) have been experimentally demonstrated to support ABCs self-assembly, restricted only by the ABCs solubility. However, it should be possible to select or create new ILs with different cation and anion combinations as self-assembly media if favorable molecular interactions between the IL and the block copolymer, which governs the self-assembly and resultant phase behavior, can be identified.

Properties of self-assembly media

Aside from high ionic conductivity and electrochemical stability, ILs have additional, remarkable properties that make them candidates for self-assembly media, including negligible vapor pressure, good chemical and thermal stability, and wide liquid temperature ranges.¹² These vastly different physicochemical properties between water and ILs is a direct consequence of very different molecular structures. Atkin^{13,14} and Hayes^{2,15-17} *et al.* have carried out systematic studies and have reviewed the literature to reveal that ILs are highly structured solvents. Further, a recent review shows that the microstructures of ILs can be modeled over a broad range of length scales, ranging from supramolecular (ion pairs, H-bonded networks, ion and clusters) to self-assembled (micelle-like, mesoscopic) solvent structures.² This difference between ILs and classical molecular liquids manifests in many ILs as a long-range disordered sponge (L_3 phase), where the ions form a network of polar and non-polar domains due to electrostatic and solvophobic clustering of like molecular groups.² This order is on the nanometer length scale and as such, may not directly influence the self-assembly of block copolymers which have mesophase structures typically an order of magnitude larger. However, this topic remains relatively unexplored. What may be important, however, is that this propensity of ILs to self-organize is due to their amphiphilic structure when not dissociated, such that ionic liquids can act as co-surfactants in molecular mesophase formation. This can lead to unique features, such as the stabilization of water nanoclusters in ILs¹⁸ or even the formation of spontaneous vesicles with a single surfactant.¹⁹

Thermodynamics and kinetics of micellization in ILs

The solution self-assembly of block copolymers may be limited by thermodynamics or kinetics. Thermodynamic considerations include the development of a phase diagram, which includes the critical micellization concentration (CMC) and critical gelation concentration (CGC), as well as the progression of equilibrium mesophases. In addition to the specific chemical composition, temperature and pressure, the polymer molecular mass and polydispersity will dictate the length scale(s) of the mesophase. Concepts traditional to surfactant self-assembly can also be valuable, such as packing parameter. Kinetic considerations arise when considering mixing and possible nonequilibrium phases, as well as the (often) slow equilibration of mesophases.

From thermodynamics perspectives, ABC solution self-assembly in solution is primarily thought to be an entropically driven process, whereby the solvent molecules surrounding the solvophobic blocks acquire a lower entropy H-bonded network configuration through self-assembly than when they are surrounded by other water molecules. The strength of this entropic driving force for a given IL is characterized through the solvent's Gordon parameter, which is a measure of cohesive energy density of the solvent. A higher Gordon parameter implies a stronger driving force for phase separation. In the mixture this translates into, a hydrophobic effect²⁰ in aqueous micellar solutions, or a solvophobic effect for ILs.²¹

Aside from this largely entropic solvophobic interaction, the chemical nature of the block copolymer and the enthalpic interactions with the IL play a critical role. This is the basis of the classic Flory χ parameter that is foundational to polymer thermodynamics (e.g., the Flory-Huggins constitutive model) and is a determining parameter in the solution and melt thermodynamics of block copolymers more broadly.

Additional factors that dictate the solution self-assembly include specific block copolymer properties (e.g., molecular mass, polydispersity, relative block lengths, primary chain configuration, chain branching topology),⁹ Such molecular properties are often coarse-grained into concepts such as the packing parameter, whereby the specific self-assembled topology is determined by a free energy balance that includes the chain stretching in the core, the inter-coronal interactions, and the excess core-corona interfacial energy.^{20,22,23} Among the various molecular considerations, the specific role of H-bonding in self-assembly is not fully understood. Hayes *et al.* report that most of the PILs form 3-D H-bond networks which are different from that in water, and are confined within the polar domain between adjacent proton donor and acceptor sites of the IL's nanostructure.² Furthermore, Hayes *et al.* argued that these H-bonds in ILs are accommodated between ions, but do not control self-assembly nor are they the principle driving force for structure formation.² However, these H-bonds are important for applications as they control the IL solvent properties and proton transfer.^{2,24}

All of these factors play a role in self-assembly, which is inherently a cooperative process that requires the simultaneous participation of numerous amphiphilic and solvents molecules and ions. As an example, the relatively simple case of surfactant micellization in water is characterized by a CMC and a critical micellization temperature (CMT). The hydrophobic effect mandates a lower micelle size limit as assemblies of low aggregation number of amphiphilic molecules cannot eliminate the unfavorable solvophobic/solvent interface, meanwhile repulsive interactions between the charged head-groups of amphiphilic molecules impose an upper size limit and restrict the micelle growth. Due to the inherent microstructure and ionic nature of ILs, as well as their inherent amphiphilic nature when they are not dissociated, the self-assembly of ABCs in ILs is inherently more complex than in aqueous solution as will be demonstrated in more detail in the next section.

The dynamics of self-assembled block copolymers, which include micellar exchange relaxation (termed as "relaxation kinetics" for non-equilibrium micelles and "equilibrium dynamics" for equilibrium micelles), and unimer to micelle formation (termed as "micellization kinetics") are often very slow in ABC assemblies in aqueous system.²⁵⁻²⁹ Because of this extremely slow dynamics, the self-assembled structure are highly dependent on assembly pathway, and the "final" morphology is often a kinetically-trapped or long-lived metastable state.²⁸ A number of experimental,^{26,27,30-32} theoretical,^{23,33-35} and computational^{36,37} research has provided valuable insights on kinetics of ABC aqueous micelles. Generally speaking, two mechanisms are found to be key for stimulating the changes in micelle size and structures, namely, single chain exchange and micelle fusion/fission. Although the role of those two mechanisms in polymeric micelle dynamics is still a subject of research, it is generally accepted that single chain exchange mechanism is dominant for micelle microstructures near equilibrium,^{26,30,33} while the fusion/fission mechanism dominates micelle growth far from equilibrium.³² Specific measurements of such kinetics for ABCs in ILs are discussed in the next section.

Microstructure-property relationships for self-assembled block copolymer/ionic liquid systems

Self-assembly of ABCs in ILs not only provides new sources of complex colloidal model systems for study, but also constitutes a platform for combining the outstanding physicochemical properties of ILs with a number of favorable attributes offered by ABCs contributing to the field of soft materials science. In particular, ABCs self-assemble into well-defined nanostructures, which can be engineered to provide a durable and stretchable mechanical scaffold for templating ILs into the self-assembled ion-conducting channels. Fundamental understanding of the structure and thermodynamics of ABCs in ILs is critical for developing microstructure-property relationship in predictable design of hierarchically structured, functional soft materials.

Dilute solutions of block copolymers in ionic liquids

Investigation of the ABCs self-assembled phase behavior in ILs typically begins with the study of micellization in dilute solution. The thermal stability and low volatility of PILs and AILs open up new opportunities to investigate the self-assembly of ABCs over a wide range of temperatures. We examine micellization for each class of IL as follows.

Micellization in protic ionic liquids

The earliest reports of ILs capable of supporting self-assembly were for PILs in 1980s, mainly belonging to the family including alkylammonium nitrate.^{38,39} The use of alkylammonium nitrate as a self-assembly medium has often been considered with reference to water, due to the evidence of similar H-bonding structures found in EAN as revealed by Evans *et al.*³⁸ Self-assembly in aqueous systems are often used to guide investigations in alkylammonium nitrate, as they are thought to have similar driving forces for micellization.⁴ As briefly mentioned in the previous section, the driving force for micellization in alkylammonium nitrate is due to the favorable solvent entropy gain from shielding the solvophobic blocks out of the polymer, which include unfavorable organization in the surrounding PIL.^{20,38} However, one of the main quantitative differences between alkylammonium nitrate and water is that the hydrocarbons in the ABCs are more soluble in alkylammonium nitrate, which results in a weaker solvophobic effect of the ILs as compared to the equivalent hydrophobic effect of water.⁴⁰ This quantitative difference leads to higher CMCs in alkylammonium nitrate, as the greater solubility in alkylammonium nitrate requires more unimers or longer ABC chains to impose similar aggregation behavior to that in water.^{41,42} To have a better look at the behavior of CMC in water versus ILs, CMC measurements for currently reported ABCs in PILs and AILs are listed in Table 1, along with the corresponding CMCs in water and other relevant self-assembly properties if available. Nevertheless, micellization in both water and alkylammonium has been shown to be a spontaneous process, with a clear discontinuity in solution properties below and above CMC, and also followed closed association micellization model,²⁰ reflecting the single step unimers to micelles equilibrium.^{4,38} However, micellization of alkylammonium nitrate in water causes an increase in partial molar volume, while no change in partial molar volume was observed in EAN, suggesting micellization process does not significantly change EAN's solvent structure.^{4,43}

Table 1: Micellization of block copolymers in ionic liquids compared to aqueous solvents.

Line	Block copolymers	Formula	M _n (g/mol)	HLB ⁴⁴	Solvents	Temp (°C)	CMC (wt%)	c (wt%)	Self-assembled morphology	Morphology geometry parameters (nm)	N _{agg} (Temp)	Ref		
1	Pluronic F127	EO ₁₀₀ -PO ₆₅ -EO ₁₀₀	12600	22	H ₂ O	20	4 ^a					45		
						25	0.7 ^a							
						30	0.1 ^a							
		EO ₁₀₆ -PO ₇₀ -EO ₁₀₆	13388	H ₂ O	35	0.025 ^a								
					40	0.008 ^a								46
					15	0.7 ^b			Spherical micelle	R=5.7 ^c	22 ^d , 37 ^c			
EO ₁₀₆ -PO ₇₀ -EO ₁₀₆	11500	d ₃ EAN	42	0.005 ^b										
					25	5			Core-shell sphere	R=7.2 ^d	9.8 ^d	47		
					31	1.8								
2	Pluronic F68	EO ₇₉ -PO ₃₀ -EO ₇₉	8400	29	H ₂ O	30	~10					48		
														49
					[BMIM][PF ₄]									
					[BMIM][PF ₆]	25	~30							
3	Pluronic P123	EO ₁₉ -PO ₆₉ -EO ₁₉	5750	8	H ₂ O	20	0.18 ^a						45	
						25	0.03 ^a							
						30	0.005 ^a							
						35	0.001 ^a							
						25	0.004 ^b							
		EO ₂₀ -PO ₇₀ -EO ₂₀	5820	H ₂ O	1	Spherical micelle	R _c =5.77 ^c	86 ^c , 93 ^d						
		EO ₂₀ -PO ₇₀ -EO ₂₀	5820	H ₂ O	3	Core-shell sphere	R _c =5.16, T= 3.58 ^e	85.6 ^d					46	
		EO ₂₀ -PO ₇₀ -EO ₂₀	5820	H ₂ O	5	Core-shell sphere	R _c =5.15, T= 3.44 ^e	85.1 ^d						
		EO ₂₀ -PO ₇₀ -EO ₂₀	5820	H ₂ O	10	Core-shell sphere	R _c =5.21, T= 3.15 ^e	88.1 ^d						
		EO ₂₀ -PO ₇₀ -EO ₂₀	5820	H ₂ O	20	Core-shell sphere	R _c =5.34, T= 2.17 ^e	94.7 ^d						
		EO ₂₀ -PO ₇₀ -EO ₂₀	6710	d ₃ EAN	15	Core-shell sphere	R _c =6.0, T= 2.07 ^e	134.6 ^d						47
		EO ₂₀ -PO ₇₀ -EO ₂₀	6710	EAN	25	Core-shell sphere	R=7.4 ^d	164 ^d						
		EO ₂₀ -PO ₇₀ -EO ₂₀	6710	EAN	3	Core-shell sphere	R _c =5.1, T= 2.17 ^e	82.6 ^c						50
EO ₂₀ -PO ₇₀ -EO ₂₀	6710	EAN	5	Core-shell sphere	R _c =5.24, T= 2.10 ^e	89.9 ^e								
EO ₂₀ -PO ₇₀ -EO ₂₀	6710	EAN	10	Core-shell sphere	R _c =5.36, T= 2.65 ^e	95.9 ^e								
EO ₂₀ -PO ₇₀ -EO ₂₀	6710	EAN	20	Core-shell sphere	R _c =5.23, T= 2.55 ^e	89.1 ^e								
EO ₂₀ -PO ₇₀ -EO ₂₀	7000	[BMIM][PF ₆]	25	Core-shell sphere	R _c =6.00, T= 2.86 ^e	51	1							
							5							
							10							
							20							
							1							
							5							
							10							
							15							
							20							
							25							
							30							
							20							
EO ₂₀ -PO ₇₀ -EO ₂₀	7000	[BMIM][FAP]	65	Core-shell sphere	R _c =5.69, T= 3.10 ^e	51	20							
							35							
							45							
							55							
EO ₂₀ -PO ₇₀ -EO ₂₀	7000	[BMIM][FAP]	20	Core-shell sphere	R _c =5.57, T= 3.10 ^e	51	20							
							20							
EO ₂₀ -PO ₇₀ -EO ₂₀	7000	[BMIM][FAP]	0-15	No evidence of micelles or any self-assembled nanostructures ^e	R _c =5.37, T= 3.56 ^e	51								
4	Pluronic P105	EO ₃₇ -PO ₅₆ -EO ₃₇	6500	15	H ₂ O	20	2.2 ^a					45		
						25	0.3 ^a							
						30	0.025 ^a							
						35	0.005 ^a							
						40	0.001 ^a							
		EO ₃₇ -PO ₅₆ -EO ₃₇	6500	d ₃ EAN									52	

5	Pluronic P85	EO ₂₆ -PO ₄₀ -EO ₂₆	4600	16	H ₂ O	25 30 35 40 45	4 ^a 0.9 ^a 0.2 ^a 0.05 ^a 0.014 ^a	Low	Gaussian coil Spherical micelle Prolate ellipsoid	R _G = 1.7 ^d R _c =4-5 ^d	37(20), 78(40) ^d	45	
		EO ₂₅ -PO ₄₀ -EO ₂₅	4500		D ₂ O	≤15 ~25 60-70						53	
		EO ₂₆ -PO ₄₀ -EO ₂₆	4600		d ₃ EAN							52	
6	Pluronic P65	EO ₁₈ -PO ₂₉ -EO ₁₈	3400		H ₂ O	30 35 40 45 50	4 ^a 1 ^a 0.35 ^a 0.1 ^a 0.04 ^a	1, 10 1 10	Gaussian coil Spherical micelle	R _G = 1.5 ±0.2, T=3.2 ^d R _G = 1.5 ^d	1 ^c 4 ^c 21 ^c 2 ^c 17 ^c	45	
		EO ₂₀ -PO ₃₀ -EO ₂₀	3500		H ₂ O	25 30 32 40	8 ^b 3.2 ^b 0.15 ^b					46	
		EO ₁₉ -PO ₃₀ -EO ₁₉	3400		d ₃ EAN	25 63 63						52	
7	Pluronic L121	EO ₅ -PO ₆₈ -EO ₅	4400	1	H ₂ O	37	0.001mM ^f	1 5 1 1, 10	Vesicles Vesicles Lamellar vesicles Lamellar stacks	R _c =30.3, T ₁ = 8.9 ^d R _c =13.2, T ₁ = 20.7, T ₂ = 77.4 ^d d~20, T _{pp0} =4.6 ^d		44	
		EO ₅ -PO ₇₀ -EO ₅	3720		d ₃ EAN	25						47	
		EO ₅ -PO ₆₈ -EO ₅	4400		d ₃ EAN	25 63						52	
8	Pluronic L81	EO ₆ -PO ₃₉ -EO ₆	2750	2	H ₂ O	37		1 1 10	Gaussian coil Lamellar stacks Polydisperse vesicle	R _H = 1.5 ^g R _G = 1.4 ^d d~18 ^d R=120, T=4.3 ^d		54	
		EO ₃ -PO ₄₃ -EO ₃	2750		d ₃ EAN	25 63 63						52	
9	Pluronic L64	EO ₁₃ -PO ₃₀ -EO ₁₃	2900	15	H ₂ O	30 35 40 45	1.5 ^a 0.4 ^a 0.1 ^a 0.02 ^a					45	
		EO ₁₃ -PO ₃₀ -EO ₁₃	2900		[BMIM][BF ₄]	24.85	0.000221 ^b mol/L					49	
10	Pluronic L61	EO ₃ -PO ₃₀ -EO ₃	2000	3	[BMIM][BF ₄]	24.85	0.0000375 ^b mol/L						49
						34.85	0.0000335 ^b mol/L						
						44.85	0.0000303 ^b mol/L						
						24.85	0.0181 ^b mol/L						
						34.85	0.0122 ^b mol/L						
44.85	0.0084 ^b mol/L												
11	PEGE-PEO	EGE ₁₀₉ -EO ₅₄	13600		D ₂ O	25			Disk Disk Disk Disk Disk	R _c > 300 ^d R _c > 300 ^d R _c > 300, T= 11 ^d R _c > 300, T= 11 ^d R _c > 300, T= 13 ^d		55	
					EAN	25							
					PAN	45							
						70							
						100							

		EGE ₁₁₃ -EO ₁₁₅	16700		D ₂ O EAN PAN	25 25 45 70 100			Core shell sphere Disk Sphere Sphere Sphere	R _c = 13, T = 7 ^d R _c > 300 ^d R _c = 10 ^d R _c = 13 ^d R _c = 14 ^d	450 200 510 679	
		EGE ₁₀₄ -EO ₁₇₈	18600		D ₂ O PAN	25 70 100			Core shell sphere Sphere Sphere	R _c = 9, T = 10 ^d R _c = 12 ^d R _c = 13 ^d	170 420 510	
12	PGPrE-PEO	GPrE ₉₈ -EO ₂₆₀	21400		D ₂ O EAN PAN	25 25 10 25 70 100			Core shell sphere Core shell sphere Sphere Sphere Sphere Sphere	R _c = 10, T = 8 ^d R _c = 12, T = 7 ^d R _c = 9 ^d R _c = 12 ^d R _c = 9 ^d R _c = 9 ^d	210 350 190 230 150 30	55
13	PS-PEO	PS-PEO PS-PEO PS-PEO PS-PEO (20-13) PS-PEO (20-13) PS-PEO (20-8) PS-PEO (20-5) PS-PEO (1-3)	28700 14100 8500 20000 20000 20000 20000		H ₂ O [BMIM][BF ₄] [EMIM][TFSA] [BMIM][BF ₄]	 0.13 ^h 0.12 ^h 0.088 ^h ~0.5	1.0 ⁱ 3.2 ⁱ , 1.6 ^h 2.8 ⁱ , 2.8 ^h Check SI		Core-shell micelle	R _H = 22 ^j R _H = 14 ^j R _H = 10 ^j		56 31 57
14	Micelle shuttle	PB-PEO (9-20) PB-PEO (9-10) PB-PEO (9-17) PB-PEO (9-4)	30200 19100 16400 13200		H ₂ O [BMIM][PF ₆] [BMIM][PF ₆] [BMIM][PF ₆] H ₂ O [BMIM][PF ₆]				Spherical micelles Spherical micelles Spherical micelles Spherical micelles Wormlike micelle Wormlike micelle Bilayered vesicle Wormlike micelle Bilayered vesicle	R _c = 22.2 R _c = 15.2 ^k , R _H = 46 ^g R _c = 18.6 ^k , R _H = 36 ^g R _c = 20.7 ^k , R _H = 54 ^g R _c = 12.0 ^k R _c = 15.8 R _c = 8.8 R _c = 14.5 ^k , R _H = 97 ^g R _c = 12.0 ^k		58,59 60 60 60 60 58,59 58,59 60 60
15	PS-PMMA	PS-PMMA (3-13) PS-PMMA (7-8) PS-PMMA (11-4)	3000 7000 11000		[EMIM][TFSA]		0.40 ^h 0.14 ^h 0.078 ^h		Core-shell micelle			31
16	Micelle shuttle	PB-PEO (9-21) PB-PEO (9-10) PB-PEO (9-17) PB-PEO (9-4)	30200 19100 16400 13200		H ₂ O [EMIM][TFSI] H ₂ O [EMIM][TFSI] H ₂ O [EMIM][TFSI] H ₂ O [EMIM][TFSI]	25 40 60 80 100 25 40 60 80 100				R _H = 74 ^g R _H = 54 ^g R _H = 55 ^g R _H = 56 ^g R _H = 57 ^g R _H = 55 ^g R _H = 61 ^g R _H = 47 ^g R _H = 46 ^g R _H = 47 ^g R _H = 50 ^g R _H = 48 ^g R _H = 95 ^g R _H = 60/61 ^g R _H = 103 ^g R _H = 71/72 ^g		61
17	LCST	PnBMA-PEO (12-9)			[EMIM][TFSA]/ [BMIM][TFSA] blends							62

					67.5/32.5 wt% 75/25 wt% 87/13 wt% 100/0 wt%	30 60 85 100				$R_H = 10^g$ $R_H = 11^g$ $R_H = 9^g$ $R_H = 7^g$	
18	LCST	PBnMA-PMMA (2.2-19) PBnMA-PMMA (7.3-19) PBnMA-PMMA (28-41)			[EMIM][NF ₂]	25 130 25 130 25 130				$R_H = 4.4^g$ $R_H = 2.5/126^g$ $R_H = 4.2^g$ $R_H = 92^g$ $R_H = 6.9^g$ $R_H = 61^g$	63
19	LCST	PS-PMMA (1.7-19)			Acetone [EMIM][NF ₂]	25 25 130				$R_H = 3.5/59^g$ $R_H = 25^g$ $R_H = 27^g$	63
20	UCMT	PEO-b-P(AzoMA-r-NIPAm)	3500		[BMIM][PF ₆]	60				$R_H = 100^g$ (under dark) $R_H = 125^g$ (under UV light irradiation)	64
21	UCMT/LCMT	PEO-PNIPAm			[EMIM][BF ₄]/[BMIM][BF ₄] blends 70/30 wt% 85/15 wt% 100/0 wt%	80 80 80				$R_H = 13^g$ $R_H = 14^g$ $R_H = 7^g$	65
22		PS-PMMA-PS	13050 11130 9760		[BMIM][PF ₆]				Spherical micelles Spherical micelles/vesicles	$R_c = 20\sim 30^l$, $R = 22.5^l$ $R < 50^l$ $R < 50^l$	66

Table 2: Thermodynamics of self-assembly of Pluronic triblock copolymers in ionic liquids compared to aqueous solvents.

Line	Block copolymers	Formula	Solvent	Temp(°C)	ΔG_m^0 (kJ/mol)	ΔH_m^0 (kJ/mol)	ΔS_m^0 (kJ/mol)	$-\Delta \Delta S_m^0$ (kJ/mol)	Ref
1	Pluronic F127	EO ₁₀₆ -PO ₇₀ -EO ₁₀₆ EO ₁₀₀ -PO ₆₅ -EO ₁₀₀	H ₂ O H ₂ O	23.1 CMT at 1wt%	-27.5	485 ^g 253 ^a	0.944		46 45
2	Pluronic F108		H ₂ O	CMT at 1wt%	-28.4	266 ^a	0.975		45
3	Pluronic P123	EO ₂₀ -PO ₇₀ -EO ₂₀ EO ₁₉ -PO ₆₉ -EO ₁₉ EO ₂₀ -PO ₇₀ -EO ₂₀	H ₂ O H ₂ O d ₃ EAN	13.7 CMT at 1wt% 22.85 23.85 24.85	-24.9	351 ^g 329 ^a 58.9 ^m 74.6 ^m 65.2 ^m	1.223		46 45 67
4	Pluronic P105		H ₂ O	CMT at 1wt%	-25.6	331 ^a	1.212		45
5	Pluronic P85		H ₂ O	CMT at 1wt%	-25.5	229 ^a	0.842		45
6	Pluronic L121	EO ₅ -PO ₇₀ -EO ₅ EO ₅ -PO ₇₀ -EO ₅	H ₂ O d ₃ EAN	17 18 20 22 25		419 ^g 32.52 ^m 38.86 ^m 65.03 ^m 74.10 ^m			46 67
7	Pluronic L64	EO ₁₃ -PO ₃₀ -EO ₁₃ EO ₁₃ -PO ₃₀ -EO ₁₃	H ₂ O [BMIM][BF ₄]	24.85	-24.5	230 ^a 21.33	0.835		45 49
8	Pluronic L61	EO ₃ -PO ₃₀ -EO ₃	[BMIM][BF ₄] [BMIM][BF ₆]	24.85 34.85 44.85 24.85 34.85 44.85	-29.35 -30.61 -31.86 -13.84 -15.31 -16.80	7.67 8.19 8.74 28.34 30.27 32.27		-37.02 -38.8 -40.6 -42.17 -45.58 -49.06	49

- The tabulated values are measured under various characterization techniques, including ^adye solubilization method, ^bsurface tension measurements, ^cstatic light scattering (SLS), ^dsmall angle neutron scattering (SANS), ^esmall angle X-ray scattering (SAXS), ^fpyrene probe, ^gdynamic light scattering (DLS), ^hI3/I1 plots, ⁱexcitation spectra, ^jquasi-elastic light scattering (QELS), ^kCryogenic transmission electron microscopy (Cryo-TEM), ^ltransmission electron microscopy (TEM), ^misothermal titration calorimetry (ITC).
- HLB (hydrophilic-lipophilic balance) values of the copolymers were determined by manufacturer.
- The morphology geometry parameters are: c is block copolymer concentration, R is overall micelle radius, R_h is the hydrodynamic radius, R_c is micelle core radius, T is overall corona thickness, d is the lamellar repeat spacing, T_1 is shell thickness of the 1st shell, T_2 is the shell thickness of 2nd shell, T_{PPO} is PPO layer thickness, N_{agg} is aggregation number.

Pluronic® is one of the most studied commercially available non-ionic block copolymers in water and ILs. The aforementioned comparable characteristics of self-assembly in water versus in PIL can be further elaborated through the example of Pluronic F127 self-assembly in water and partially deuterated ethylammonium nitrate (d_3 EAN). As shown in Figure 1, both Pluronic F127/water and Pluronic F127/ d_3 EAN systems have similar phase behaviors originating from the similar self-assembly driving force, where spherical micelles form at low concentration and those micelles further self-assemble into a cubic and crystal phases at elevated concentration and temperature.^{46,47} As tabulated in Table 1, the micelle sizes in both systems are of the same order of magnitude, but CMC values and aggregation numbers are 2 orders of magnitude larger in d_3 EAN than in water. A significant lowering of ΔG_m^0 in Table 2 indicates the lower solvophobicity of the solvophobic blocks of the polymer in d_3 EAN as compared to water. Interestingly, similar results were obtained when comparing the self-assembly of Pluronic F68 in water versus AIL.⁴⁹ This was attributed to the much weaker driving force in d_3 EAN. Utilizing small angle neutron scattering (SANS) and combining with mass balance, López-Barrón *et al.* proved that there are less than 10 vol% of d_3 EAN in the spherical micelle core formed by Pluronic F127.⁶⁸ Compared to self-assembly in water,⁶⁹ this extremely low degree of solvent penetration in the micelle core verified the weaker segregation strength in d_3 EAN.

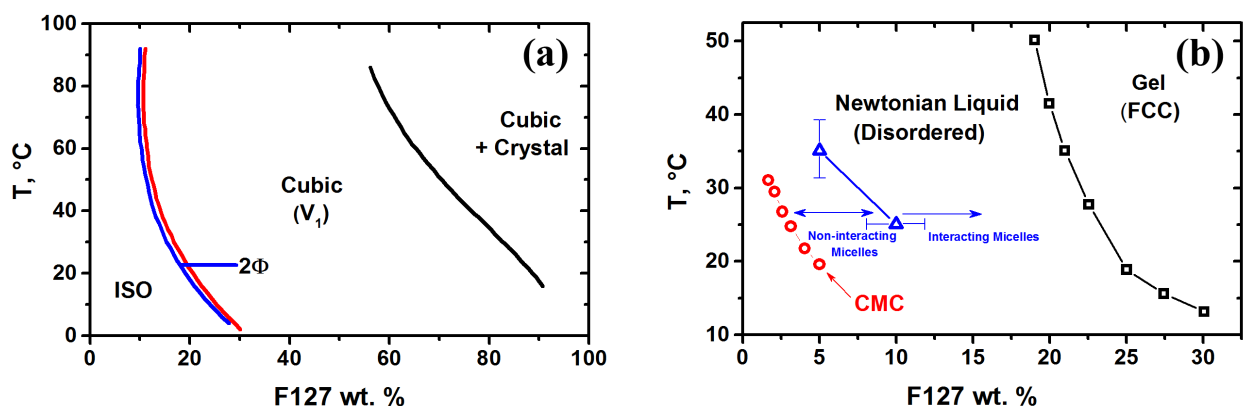


Figure 1: (a) Phase diagram of Pluronic F127 in water. The figure was adapted from⁴⁶. Reprinted with permission from⁴⁶. Copyright © 1994, American Chemical Society. (b) Phase diagram of Pluronic F127 in d_3 EAN. The figure was reproduced from⁴⁷. Reprinted with permission from⁴⁷. Copyright © 2014, American Chemical Society.

To interrogate the effect of relative solvophilic to solvophobic block size on the self-assembled microstructure, the microstructure and rheological properties of micellar solutions of a homologous series of Pluronics with similar PPO block, F127, P123 and L121, in d_3 EAN were studied.⁴⁷ In analogy to aqueous solutions, the larger PEO/PPO molar ratios promotes the formation of spherical micelles, whereas small PEO/PPO ratios favor the formation of less curved microstructures, such as vesicles, wormlike micelles (WLMs), and lamellar phases. The CMCs for Pluronics F127 and P123 show LCST-like CMC behavior, but at much higher concentrations than observed in water. These micelles develop strong intermicellar interactions upon increasing the Pluronic concentration, and further increase in concentration or temperature results in an order–disorder transition to a supramolecular cubic microstructure (FCC for F127 and BCC for P123) with a gel-like rheological behavior, as shown in their corresponding phase diagrams in Figure 1(b) and Figure 2(a). Utilized SANS, ultra-small angle neutron scattering (USANS) and confocal microscopy, it was found that Pluronic L121 exhibits a much richer phase diagram, as shown in Figure 2(b)-(g).

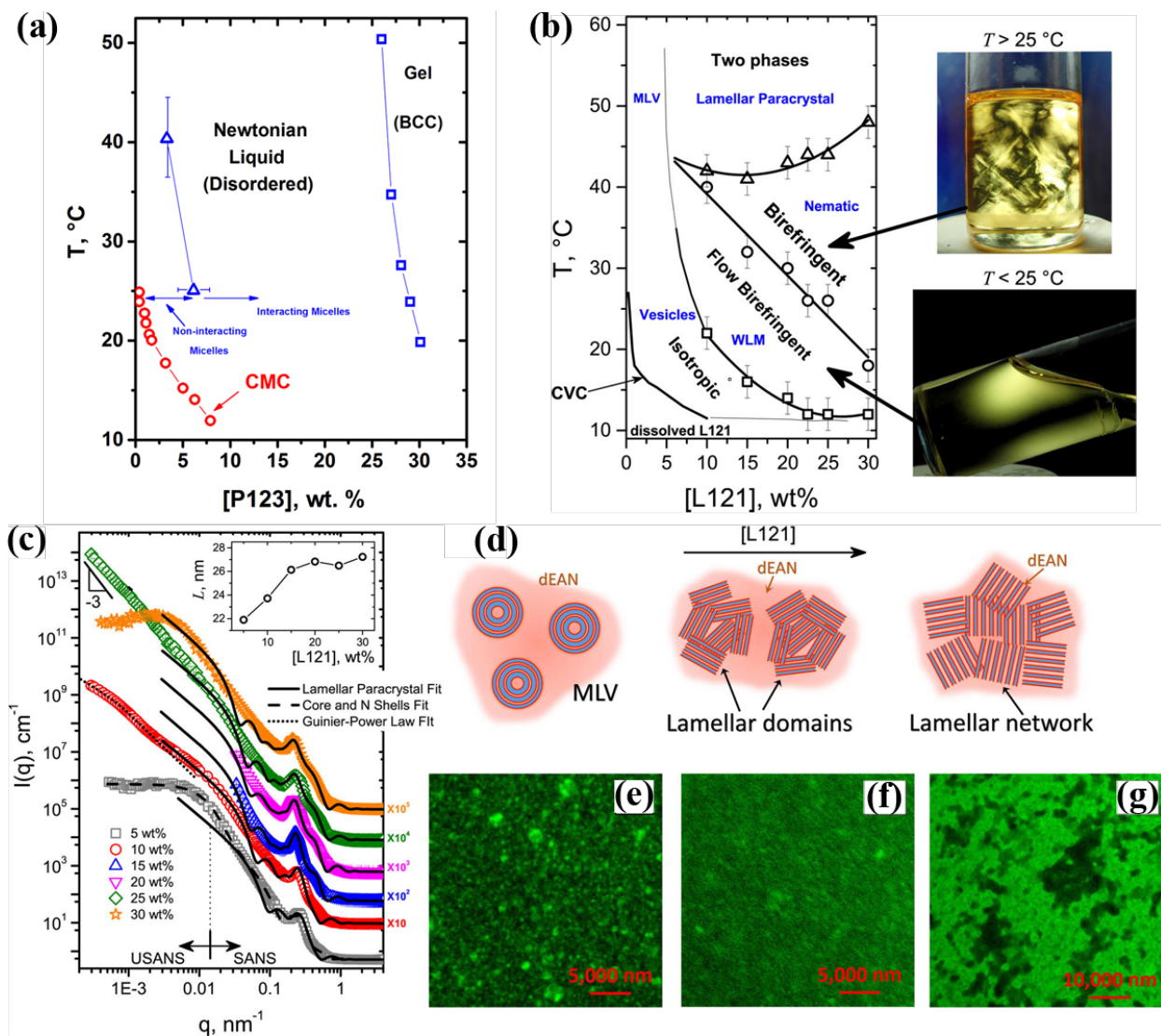


Figure 2: (a) Phase diagram of Pluronic P123 in d_3 EAN. (b) Phase diagram of Pluronic L121 in d_3 EAN. Right panel: photographs of vials containing a 25 wt % LdE solution at $T < 25$ °C (showing flow induced birefringence) and at $T > 25$ °C (showing permanent birefringence). (c) Combined SANS and USANS from Pluronic L121 in d_3 EAN solutions with the indicated compositions, measured at 60 °C. Solid, dashed, and dotted lines are best fits to the lamellar paracrystal, the core with N shells, and the Guinier–Porod models, respectively. Data are shifted by multiplying by the indicated factors for clarity. (d) Schematics of the transitions from multilamellar vesicles to disperse lamella domains to lamella networks, upon increase of concentration. (e), (f), and (g) show confocal micrographs (taken at 60 °C) of 10, 25, and 30 wt % Pluronic L121 in d_3 EAN solutions, respectively. The figure was reproduced from ⁴⁷. Reprinted with permission from ⁴⁷. Copyright ©2014, American Chemical Society.

Micellization in aprotic ionic liquids

The use of AILs as self-assembly media is relatively more recent, whose history could be dated to 2003⁷⁰. To investigate the microstructure of amphiphilic block copolymer self-assembly in AILs, Lodge and co-workers conducted a comprehensive study on a series of carefully selected diblock copolymers/AIL model systems, including PB-PEO/[BMIM][PF₆],⁶⁰ PS-PEO/[EMIM][TFSA],³¹ and PS-PMMA/[EMIM][TFSA].³¹ The PB-PEO/[BMIM][PF₆] model system formed self-assembled nanostructures consisting of micelles: insoluble dense PB cores surrounded by well-solvated PEO coronas. Combining direct visualization of micelles via cryo-TEM (Figure 3) with DLS measurements, Lodge *et al.*

revealed that decreasing the solvophilic PEO molecular weight (MW) resulted in universal nonergodic micellar morphology, ranging from spherical micelles, WLMs, to bilayered vesicles.⁶⁰ This nonergodicity effect is attributed to strong amphiphilicity and relatively low solvent compatibility of block copolymers. The observed structural changes resulting from the variation of copolymer composition qualitatively resembles that observed in water.^{25,59} With this prior knowledge in mind, the effect of block copolymer MW and composition on CMC were examined on two well-defined and systematically prepared model systems: PS-PEO (varying solvophilic PEO MW, maintaining solvophobic PS MW) and PS-PMMA (varying solvophobic PS MW, maintaining overall MW) in [EMIM][TfSA]. Literature suggests a strong CMC dependence on solvophobic block MW at lower MW, but a weaker dependence at higher MW. However, it was found that both systems shows a very weak CMC dependence on solvophobic molecular weight. The authors hypothesized that this discrepancy results from the collapse of unimer solvophobic blocks and potential role of kinetic limitations.

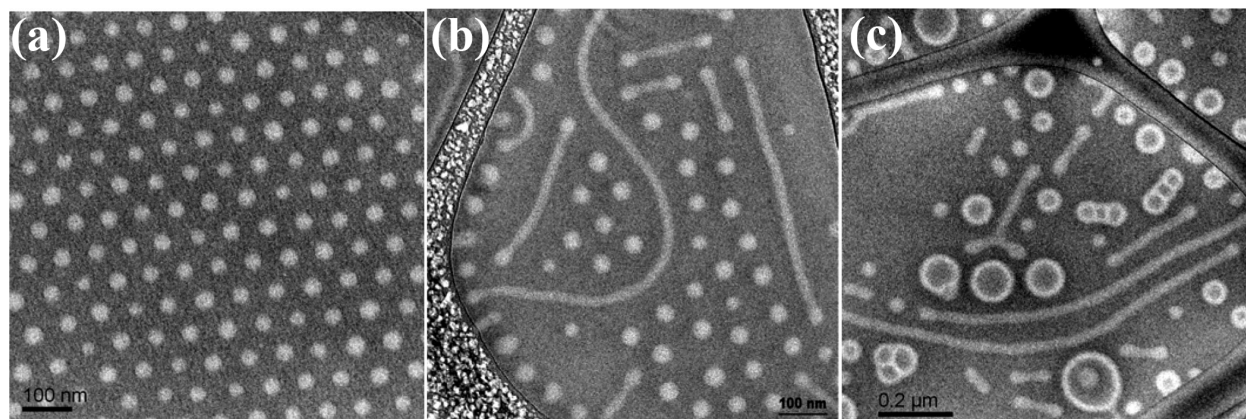


Figure 3: Cryo-TEM images for 1 wt% PB-PEO self-assembly in [BMIM][PF₆] solutions. (a) Bright circles, (b) bright strings, (c) bright double layered circles correspond to spherical micelles, cylindrical micelles, and bilayer vesicles, respectively. And PB lies in the micelle cores. The figure was reproduced from⁶⁰. Reprinted with permission from⁶⁰. Copyright @2006, American Chemical Society.

Following up with the dynamics and equilibrium and non-equilibrium microstructure alluded in the previous section, the nonergodic morphology, formation and relaxation kinetics, equilibrium and non-equilibrium micellar structures, as well as effect of preparation methods on self-assembly of ABC micelles in ILs was investigated by Meli *et al.*^{71,72} The model system used for this study was carefully prepared PB-PEO or PS-PEO micelles in [EMIM][TFSI] or [BMIM][TFSI] using two preparation protocols: direct dissolution (ABC is directly dissolved in ILs) and cosolvent-aided dissolution (ABC and IL are dissolved first in a cosolvent followed by evaporating off the cosolvent). It was observed that steady state micelle structure are highly path dependent and consistent when changing the length of PEO corona block, the chemistry of the core block (from PB to PS), and the length of alkyl chain in imidazolium cation (from ethyl to butyl). Direct dissolution results in large and polydisperse aggregates that relax upon thermal annealing at high temperatures into smaller and monodisperse steady state spherical micelles. The rate of relaxation increases with increasing copolymer concentration, suggesting that fusion/fission is the main micelle relaxation mechanism prepared using this method. However, cosolvent-aided dissolution leads to smaller and monodisperse micelles that retain their size upon prolonged thermal annealing. These smaller spherical micelles are attribute to the lower interfacial energy between the PB or PS cores and the IL/cosolvent mixture compared to the IL alone. Kinetic stability can be derived from the steric stability of the well-solvated corona.

As mentioned in the previous section, micellization could be affected by external stimulus, such as temperature. Due to the diversity of ILs chemistry, which can be used for tuning the temperature dependent solvent quality for various polymers, many block copolymer micellar systems have been found to display interesting thermo-responsive behavior in ILs. Using homopolymer/IL system as an initial reference point,

both upper critical solution temperature (UCST) and lower critical solution temperature (LCST) phase behavior have been reported: homopolymers exhibiting UCST phase behavior in IL are PNIPAm in [EMIM][TFSA];⁷³ LCST phase behavior in ILs are PBzMA and its derivatives in [C_nMIM][TFSA]⁷⁴ and [EMIM][NTf₂],^{40,75} PEGE in [EMIM][TFSA],⁷⁶ PnBMA in [C_nMIM][TFSA]⁶² and PEO in [EMIM][BF₄],^{77,78} [BMIM][BF₄],⁷⁷ [EMMIM][BF₄]⁷⁸ and [EMIM][BF₄]/[BMIM][BF₄] blends.⁷⁷ One common characteristic of these UCST or LCST homopolymer/IL systems is that they all show asymmetric temperature-composition phase diagrams, with the critical composition shifted to low polymer concentrations excluding the case of PEO/AIL.⁷⁸ It was postulated that hydrogen bonds between polymer/IL provide the driving force for the LCST phase behavior.^{76,78} Combing those homopolymers with different phase behavior could produce thermo-responsive amphiphilic block copolymers with upper critical micellization temperature (UCMT) (both blocks are consisted of UCST homopolymers), lower critical micellization temperature (LCMT) (both blocks are LCST homopolymers), and doubly thermos-sensitive block copolymer having both features (one block is UCST homopolymer and one block is LCST homopolymer). The characterization of two thermo-responsive diblock copolymers micellar systems, PEO-PNIPAm/IL and PEO-PnBMA/IL, showed that using IL blends as solvents the UCST and LCST phase behavior could be easily tuned over a wide range of temperatures by manipulating the blending ratio of two ILs, without modifying the chemical structure of the copolymers.^{62,65} This finding points out an additional material design strategy of simply changing the IL properties through changing the chemical structures of IL constituents or by blending different ILs,^{74,77} without the complexity of changing ABCs properties or customizing new ABCs. The discovery UCST or LCST phase transition of block copolymers has been utilized in creating light controlled reversible micellization,⁶⁴ doubly thermos-sensitive micellization-unimer-inverse micellization self-assembly mechanism,⁷⁹ micelle shuttle systems,⁶¹ physical ion gel,⁸⁰⁻⁸² thermoreversible block copolymer ion gels⁸³ and the long-range-ordered regulation of ion paths by using polymer/IL composite films.⁸⁴

With the findings of nonergodic core-shell micellar nanostructures in ILs and LCST and UCST phase behavior in block copolymers, smart thermo-responsive micellar systems exhibiting spontaneous intact round-trip shuttling^{61,85} between a hydrophobic AIL and a phase-separated aqueous phase have been explored. This research topic is significant because micelle shuttle with tunable micelle size and nanostructures may supply a simple, flexible, and scalable round-trip delivery system that has potential applications in nanoencapsulation,⁸⁶ phase transfer,⁸⁷⁻⁸⁹ and biphasic catalysis^{90,91} involving ILs. Increasing research efforts in this area has experimentally confirmed the phenomena with three custom-synthesized diblock and a commercially available inexpensive triblock copolymer micellar systems in two IL/water media, which are PB-PEO,⁸⁵ PNIPAm-PEO,⁹² PNonOx-PEtOx⁹³ and P123⁹⁴ micelle shuttle between [Bmim][PF₆] and H₂O, and PB-PEO between [EMIM][TFSI] and H₂O.⁶¹ Generally speaking, the micellar shuttle mechanisms are fully thermoreversible, repeatable and quantitative, with preservation of micelle size and structure between the two solvents. From material design perspective, the design of such a micellar shuttle system requires a polymer (PEO in this case) that is nearly equally soluble in two immiscible solvents (water and AILs in this case).⁸⁵ The driving force for the thermo-controlled micelle shuttle is the well-known LCST phase behavior (solubility decreases upon heating) of PEO⁹⁵ corona block in water. As the relative affinity of the two solvents to the corona chains is temperature dependent, the solvent quality of water for PEO is deteriorated at elevated temperature, whereas the AILs remains as a good solvent. This underlying physics was fully manifested in experimental observed micelle shuttle mechanism, where micelles transfer spontaneously from aqueous phase at room temperature to both phases at the transfer temperature, and finally reside in the hydrophobic IL phase at elevated temperature.⁸⁵ To be noted, the thermodynamics and mechanism of micelle shuttle was studied using doubly-thermosensitive PNIPAm-PEO diblock copolymers in [Bmim][PF₆]. Aside from the LCST phase behavior of PEO-corona in water, the PNIPAm-core has a LCST phase behavior in water yet an upper critical solution temperature (UCST) phase behavior in [Bmim][PF₆].⁷³⁻⁷⁶ This doubly-thermosensitive micelle shuttle system achieved the goal of controlling loading and unloading in both phases and creating a more advanced reversible micellization-transfer-demicellization shuttle mechanism shown in Figure 4.⁹² Therefore, the transfer property can be effectively controlled and tuned by changing the relative solubility of PEO in water and ILs, such as adding

additives to the aqueous phase to adjust the solubility of PEO in water.⁶¹ using hydrophobic AILs with varying anions or cations to tailor the solubility in AIL or synthesizing multi-thermosensitive block copolymers with PEO-corona. With this prior knowledge as a basis, PB-PEO vesicles in water with interiors filled with [EMIM][TFSI]⁹⁶ and [EMIM][TFSA]⁹⁷ were also successfully designed.

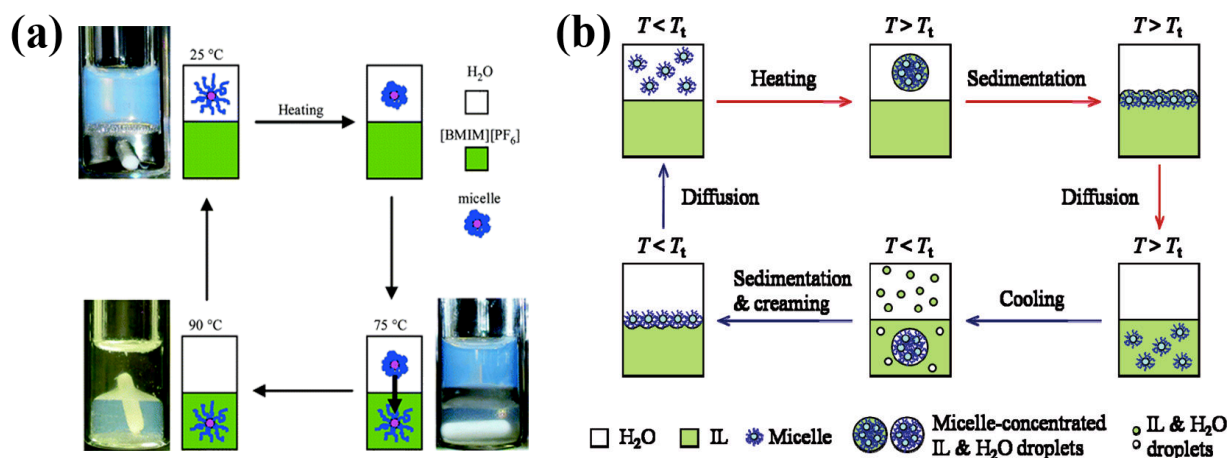


Figure 4: (a) Schematic illustration of the round trip PB-PEO micelle shuttle between [BMIM][PF₆] and water. The figure was reproduced from ⁸⁵. Reprinted with permission from ⁸⁵. Copyright ©2006, American Chemical Society. (b) Schematic illustration of mechanism of the micelle shuttle. The figure was reproduced from ⁹⁸. Reprinted with permission from ⁹⁸. Copyright © 2009, American Chemical Society.

Summary and outlook

Even though the micellization features of ABCs in PILs and AILs are often qualitatively consistent with comparable observations in aqueous solutions, the low volatility and tunable solvent properties of ILs allow for new examinations of significant quantitative differences in the self-assembly behavior over a wide range of temperatures. Since the micellization of ABCs in ILs is still a developing field, many interesting areas are still waiting to be conquered and can be summarized from three perspectives. From the perspective of polymer thermodynamics relating to closely to micelle structure and thermodynamics, the applicability of mean-field theories and scaling theories in morphology control has not yet been thoroughly explored. From the viewpoint of micelle dynamics, given that ABCs can form equilibrium or non-equilibrium microstructures depending on the solution preparation methods, so a coherent understanding of micelle dynamics during micelle formation and structural transitions, as well as careful optimization of the preparation conditions are critical for formulating and processing well-defined, uniform and reproducible microstructures.^{28,29} Lastly, achieving controllable stability in the self-assembly is also an important subject for desired applications. Indeed, given the reported phase diagrams and material design properties of ABCs in ILs, controlling the self-assembly of these systems will open up new opportunities for formulating hierarchical structured soft matter, as discussed further in the next section.

Concentrated solutions of block copolymers in ionic liquids

Concentrated solutions of ABCs in IL have more diverse phase behavior than dilute solutions. At fixed temperature, the addition of IL to ABCs results in a rich sequence of lyotropic phase transitions due to the multiple independently varying interaction parameters (interactions between the amphiphilic blocks and the interactions between blocks and solvents) present in binary or multi-component systems. The temperature dependence of those interaction parameters results in thermotropic phase transitions. However, work in this field has been much less explored compared to the investigations of dilute solution self-assembly.

Microstructure-property relationship in quiescent state

The lyotropic phase behavior of concentrated ABCs/IL mixtures resembles that of mixtures of ABCs in selective molecular solvents. Due to the selectivity of the selective solvent to solvophilic block(s), the factors affecting lyotropic phase behavior of ABC in selective solvents are the relative volume fraction of solvophilic (or solvophobic) block(s) in ABC, volume fraction of ABC in mixture and the selectivity of the solvent.⁹⁹ It was nicely demonstrated by Lai *et al.* that order-disorder transition temperature and domain spacing of the ordered morphology decreases with increasing solvent concentration when solvent selectivity is small, and increases with increasing solvent concentration when solvent selectivity is large.¹⁰⁰ Further the domain spacings have been shown to follow a scaling law parametrized by volume fraction of ABC in mixture, solvent selectivity and the morphology.¹⁰¹ The driving force for the lyotropic mesophase transitions induced by the addition of a selective solvent is the combination effect of changes in the effective volume fractions of each phase and degree of segregation between domains.^{99,102}

Concentrated solutions of block copolymers have similar self-assembled microstructures as the bulk state.^{9,103} The commonly found microstructures in diblock copolymers bulk states include cubic lattices of spheres (either BCC or FCC), hexagonally packed cylinders (HEX), the bicontinuous gyroid (G), and lamellae (LAM).¹⁰³ The lyotropic phases observed in four diblock copolymer/AIL model systems are PB-PEO in [EMIM][TFSI] or [BMIM][PF₆] (BCC, HEX, LAM, regions of coexistence of LAM and HEX, and a disordered network structure consisting of branched PB cylinders in a matrix of PEO/ILs),¹⁰⁴ PS-PEO/[EMIM][TFSI] (G, coexistence between LAM and G, coexistence between LAM, HEX and G microphases and coexistence of LAM phases with two different domain sizes),¹⁰² and PS-P2VP/[Im][TFSI] (BCC, FCC, HEX, LAM, coexistence of LAM phases with two different domain sizes).^{105,106} In these systems, the AILs selectively solvate the solvophilic PEO or the P2VP blocks of the copolymers, resulting in the lyotropic phase behavior. These interesting coexistence phase was proposed to be caused by two lamellar phases contain unequal amounts of ionic liquid, or perhaps due to cocrystallization of the polymer and ionic liquid in the case of the PS-PEO/[EMIM][TFSI]. The coexistence of G microphase in PS-PEO/[EMIM][TFSI] was attributed to the strong segregation strength of those systems. Further, the reported domain spacing scaling law also applied in PS-PEO/[EMIM][TFSI] and PS-PEO/[BMIM][PF₆] systems, revealing that [EMIM][TFSI] is a less selective solvent than [BMIM][PF₆].¹⁰⁴

On the other hand, with the favorable interaction between AIL [BMIM][PF₆] and PEO block, concentrated triblock copolymers Pluronic F127, F108 and F77 in [BMIM][PF₆] demonstrate their ability to form ordered morphologies.¹⁰⁷ Further increasing IL concentration activates the order-to-order transition from cylindrical to spherical PEO microdomains, as well as a large melting point depression of the PEO blocks. However, blending [BMIM][PF₆] with these Pluronic copolymers shows no signs of liquid crystals formation, which is very different from previous work with P123/[BMIM][PF₆]¹⁰⁸ and P123/EAN¹⁰⁹ and later work of Pluronic P123 and F127/d₃EAN,⁴⁷ where the formation of liquid crystalline phases is manifested by the birefringent textures when observed under a polarized optical microscope.

The model system for studying concentrated solutions of ABCs in PILs is Pluronic in EAN. Concentrated P123/EAN was identified to contain a series of lyotropic mesophases including normal micellar cubic (I₁) (FCC in this case, 28-30% P123), normal hexagonal (H₁), Lamellar Phase (L_α), and reverse bicontinuous cubic (V₂) using SAXS and optical microscopy.¹⁰⁹ Such self-assembly behavior of

P123 in EAN is similar to those observed in H₂O²² or [BMIM][PF₆]¹⁰⁸ systems except for the presence of the V₂ phase in EAN and the absence of the I₁ phase in [BMIM][PF₆]. The additional V₂ phase in P123/EAN system was hypothesized to be owing to the lower solvophobicity of the PPO blocks to EAN than to water, which might reduce the effective area of the solvophilic headgroup and increase the volume of the solvophobic part. Furthermore, similar lyotropic phase behavior observed in EAN, H₂O and [BMIM][PF₆] suggests that those three solvents have similar solvent properties in their roles both as self-assembly media and PEO solvation.

Taking a detailed look at the I₁ regime, McConnell and co-workers used a series of PS-PI diblock copolymers in decane (preferential solvent for PI) to demonstrate that FCC lattices are favored in the limit of thin micelle corona, whereas BCC crystals are preferred in systems with thick corona.¹¹⁰ These results are expected with the observation that micelles with thin coronas resemble hard spheres, and micelles with large coronas should be considered to be soft spheres.⁴⁷ With this information in mind, compared concentrated Pluronic P123 (thinner corona) and F127 (thicker corona) self-assembly in solution, the formation of FCC lattice should be anticipated for P123, as consistent with P123/EAN¹⁰⁹, and BCC lattice for F127. However, unexpected observations of FCC lattices in F127/d₃EAN⁴⁷ and F127/D₂O,¹¹¹ BCC lattices in P123/d₃EAN⁴⁷ were obtained. However, using a purified commercial F127, Mortensen et al. observed a BCC phase in concentrated F127/D₂O.¹¹¹ It was postulated that the dissolved F127 chains may form unimer clusters (as previously shown in PEO/D₂O and Pluronic/ D₂O solutions) that fill the intermicellar space and enhance stability of FCC lattice by interacting with PEO corona.⁴⁷ Therefore, it was concluded that the diblock impurity within the commercially purchased triblock copolymers and/or partial solubility promotes the formation of a FCC lattice ordering by hardening the intermicellar potential.⁴⁷ The origin of the unexpected BCC phase for P123 is still unexplained.

With these prior knowledge about concentrated systems of neat P123 and F127 in d₃EAN⁴⁷ and co-micellization of these two ABCs,¹¹² seven concentrated mixtures of P123 and F127 in d₃EAN, ranging from “hard-sphere like” P123 with BCC microstructure to “soft” with FCC microstructure at quiescent state, were used to form a series of concentrated solutions with tunable rheological signatures.¹¹³ It’s worthwhile to mention that 90/10 PFdE marked the supramolecular equilibrium microstructure transition from BCC micellar crystals (P123/d₃EAN) to FCC micellar crystals (F127/d₃EAN). Therefore, it was concluded that co-micellization could be used as a potentially means to trigger the BCC-to-FCC transition evidenced by SANS.

Thermotropic phases in concentrated ABCs/IL have also interesting properties. Hamley *et al.* showed that the thermotropic properties of PS-PI in diethyl phthalate is due to the temperature dependence on polymer/solvent interaction parameter or solvent selectivity.¹⁰¹ The previously mentioned temperature dependent scaling law in PS-PI/decane system was originated from the effect of temperature on the solvent selectivity, attributing to the changes in solvent partitioning between the PS and PI microphases as temperature varies.¹⁰¹ Systematic investigation of Pluronics in water has led to the observation of strong temperature dependence of micelle formation in these systems.²² This strong temperature dependence is depicted by the thermotropic behavior of Pluronic L121 (10-30 wt%) in d₃EAN, where reversible phase transitions from vesicles, WLM, nematic to lamellar paracrystalline phase could be observed upon heating and concentrated Pluronic P123 or F127 in d₃EAN, where BCC or FCC to disordered micellar phases could be achieved by lowering temperature, termed “inverse melting”.^{47,114} The thermotropic phase behavior in PS-P2VP/[IM][TSFI] system is described by the irreversible transitions from ordered LAM, HEX, or coexisting LAM/HEX phases to disordered micelles upon heating around 250 °C, while neat PS-P2VP demonstrates a reversible order-disorder transition around the same temperature.¹⁰⁶

Microstructure-property relationship under flow deformation

As noted, processing can be critical for achieving a desired nanostructured morphology in ABC/IL systems. Hence, fundamental studies of processing effects are of significant value. In particular, shear flows can be particularly effective for creating long-range ordering and orientation under specific conditions. In addition, self-assembled polymers in solutions also constitute an excellent soft colloidal model system,

which can often exhibit remarkable rheological responses to imposed flow fields. This originates in part from their ability to undergo conformational changes and elastic deformations, as well as the effects of deformation on their dynamical behavior. The wide range of macroscopic rheological behavior observed is a consequence of changes in the underlying microstructure that can span mesoscopic to nanoscale organization. Most prevalent to date is research investigating the microstructure of micellar cubic crystals in molecular solvents under steady shear flow. Progress in the experimental capability of measuring the microstructure-property relationship has been aided by the development of a large number of real and reciprocal space techniques qualified in simultaneously measuring microstructural and rheological properties (see, for example, the reviews by Walker¹¹⁵ and others on rheo-SANS¹¹⁶). The experimental studies for ABC/IL can be broadly categorized into two main topics, which are the exploration of the shear-induced order-order transitions, at low shear rates and understanding of the crystal shear-melting at high shear rates.^{114,117-122} The characteristic rheological response of FCC micellar crystals in molecular solvents under steady shear flow is shear thinning, originating from the formation of two-dimensional hexagonal close-packed (HCP) layers, which can orient to as to have glide planes commensurate with laminar shear flow, thus facilitating flow.¹²³ Furthermore, the HCP layers are arranged with layers normal parallel to the velocity gradient direction and the close-packed direction parallel to the velocity direction.^{121,124} Those general flow and microstructure behaviors of micellar crystals were also found in dispersions of charged colloids¹²⁵ and single component “nearly hard” colloidal spheres.¹²³ To measure the HCP layered structures, most of those studies have utilized small angle scattering experimental techniques to measure the HCP layers only in one of the three-dimensional planes, the velocity-vorticity (or 1-3) plane of flow. In this plane of flow, the in-plane HCP layered structure is visualized as a sixfold symmetric scattering pattern in reciprocal space. However, since this plane is perpendicular to the HCP layers, the information about layer staking sequence could not be obtained.

Similar studies of the microstructure under flow for self-assembled ABC/IL solutions are still rare and include two primary systems, micellar crystals and WLM IL solutions. Viscoelastic block copolymer micellar cubic crystals in ILs are formed by hierarchical self-assembly of ABCs into spherical micelles that further order into micellar crystals at sufficiently high concentrations or temperatures (Pluornic F127 FCC micellar crystals in d₃EAN).¹²⁶ In that work, a combination of rheo-SANS¹²⁷ (Figure 5(a), measuring 1-3 and 2-3 planes of flow) and spatially resolved flow-SANS¹²⁸ (Figure 5(b), measurements in the 1-2 plane of flow) were utilized to investigate the flow-induced crystallization, HCP layering and shear melting of the micellar crystals under steady shear flow.¹²⁶ In addition, time-resolved oscillatory rheo-SANS (tOrSANS, measuring 1-3 plane of flow) was used to quantify the cyclic melting and recrystallization process under large-amplitude oscillatory shear (LAOS) flows.¹²⁹ As shown in Figure 5(d), the microstructure-property relationship during the flow-induced crystallization, HCP layers formation and sliding, as well as the shear melting processes in PIL are in qualitative agreement with the behavior in molecular solvents, charged colloids and hard sphere systems. The highlight of this work is the 3D microstructure measuring capability pictured in Figure 5(c), in addition to the commonly measured 1-3 plane of flow, the measurement on the 2-3 plane of flow provide information about the stacking sequence in the shear-induced HCP layers, and the gap-resolved measurements on the 1-2 plane of flow reveals the microstructural homogeneity across the measuring gap during shear flow. With the gap-resolved 1-2 flow-SANS measurements, crystal melting and HCP layer sliding was confirmed to be non-uniformly across the gap, which suggests the existence of an inhomogeneous shear rate distribution in the gradient direction. The LAOS measurements reveal the microstructural origins of the intracycle strain-stiffening and the intra-cycle shear-thinning, which was found to originate from the extremely slow relaxation of the micellar gel, similar to concentrated hard-sphere suspensions and colloidal gels.

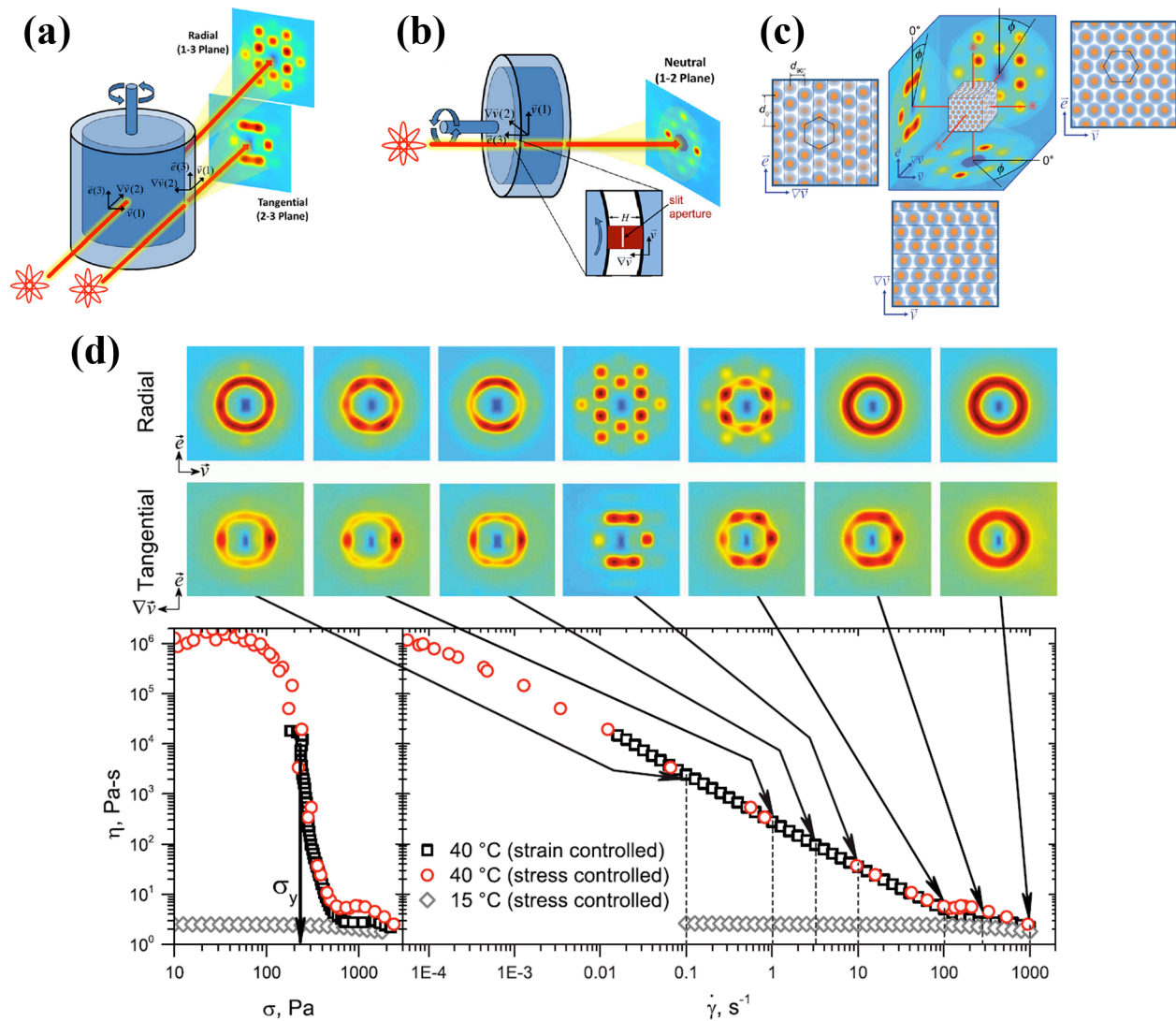


Figure 5: Schematic diagrams of (a) the rheo-SANS and (b) the flow cell. Both devices have Couette flow geometry with rotating inner cylinder. The beam in (a) is directed both in the radial and tangential directions, perpendicular to the 1–3 and 2–3 planes of flow, respectively. In (b), the beam is directed perpendicular to the 1–2 plane of flow and is reduced to a 0.1mm wide slit via a cadmium slit aperture for spatial resolution. (c) Schematic cartoon of the three-dimensional layered HCP structure and the corresponding 2D scattering profiles in the three perpendicular planes of flow obtained by shearing a 24 wt. % F127/dEAN solution with a shear rate of 10 s^{-1} . (d) Steady rheo-SANS data from 24 wt. % F127/dEAN solution measured at 40 °C. Lower panel: Steady shear viscosity versus stress and versus shear rate. Both strain-controlled measurements (black squares) and stress-controlled measurements (red circles) are shown. Viscosity data measured at 15 °C. (gray diamonds) are included for comparison. Upper panel: 2D SANS patterns measured at the shear rates indicated by the arrows in the radial and tangential direction, corresponding to the flow-vorticity ($\mathbf{v} - \mathbf{e}$ or 1–3) and the gradient-vorticity ($\nabla \mathbf{v} - \mathbf{e}$ or 2–3) planes of flow, respectively. The figure was reproduced from ¹²⁶. Reprinted with permission from AIP Publishing LLC.

Surfactant WLM solutions, which have been extensively reviewed,^{130–133} are “living” polymers, where continuous random breakage and reformation lead to a Poisson distribution of length scales at equilibrium for simple cases. This results in Maxwellian viscoelasticity in the limit where breakage is significantly more rapid than relaxation process. However, non-ionic block copolymer wormlike micellar aqueous solution have comparatively long lifetimes, which is manifested by the non-equilibrium size distribution of WLMs.¹³² Such solutions can also exhibit flow instabilities, such as shear banding, with the addition of salts.¹³⁴ Recently, investigations have been performed for a non-ionic block copolymer WLM solution in ILs comprised of Pluronic L121 in d_3 EAN, which was reported to exhibit flow birefringence and shear

thinning (Figure 2(a)).⁴⁷ To interrogate the relationship between self-assembled WLM microstructures and non-linear rheology, further work is required to explore the nature of the rheological properties of these long-threadlike micelles and the qualitative and quantitative differences and similarities to the more heavily studied surfactant WLMs. The exploration of the structure-property relationships briefly summarized here serves as a reference for formulating and processing non-ionic WLMs in ionic liquids to achieve specific structures. It also provides insights useful for further applications in synthesis of iono-elastomers via crosslinking block copolymer WLMs in ILs, as discussed next.

Summary and outlook

Concentrated ABC/IL solutions self-assemble and order into a rich variety of lyotropic and thermotropic phases in the quiescent state with a broad range of rheological properties. Under simple shear flow, these systems undergo many of the transitions observed for ABC in molecular media as well as for surfactant solutions. ABC/IL concentrated structured systems can exhibit soft solid behavior and it has been demonstrated that shear can be used to anneal, orient, melt, and even create phases nonexistent at equilibrium.¹²⁹ However, these studies are at an early stage and there are many issues waiting to be explored. A major issue already discussed in the context of dilute ABC/IL micellar solutions, i.e., whether equilibrium is achieved and the role of non-equilibrium microstructures, path dependent microstructures, and long-term stability issues, is even more relevant when considering the role of processing on these processes. For example, a better understanding of kinetic versus thermodynamic driving forces for self-assembly in concentrated ABCs/ILs may allow for more control over the self-assembly in these complex systems,⁹⁹ which is valuable for controlling the morphology of ion gels or membranes under static and deformations, as described in the next section.

Table 3: Concentrated solution of block copolymers in ionic liquids.

Line	Block copolymers	Formula	M _n (g/mol)	Solvents	Temp (°C)	c (vol %)	c (wt%)	Self-assembled morphology	d-spacing (nm)	Ref
1	Pluronic F127	EO ₁₀₆ -PO ₇₀ -EO ₁₀₆	12600	[BMIM][PF ₆]	70~80		40	Well-ordered microdomains in the melt	d-spacing = 14 ^e	107
2	Pluronic F108		14600	[BMIM][PF ₆]	70~80		40	Well-ordered microdomains in the melt	d-spacing = 14 ^e	107
3	Pluronic F77		6600	[BMIM][PF ₆]	70~80		10	Well-ordered microdomains in the melt	d-spacing = 8 ^e	107
4	Pluronic P123	EO ₂₀ -PO ₇₀ -EO ₂₀	7000	H ₂ O	25		~30	<i>I</i> ₁		135
					25		40-50	<i>H</i> ₁		
					25		65-85	<i>L</i> _α		
					25		45		lattice-spacing = 13.57 ^e	108
					25		50		lattice-spacing = 13.58 ^e	
					25		68		lattice-spacing = 12.11 ^e	
					25		75		lattice-spacing = 11.58 ^e	
					25		85		lattice-spacing = 10.94 ^e	
				[BMIM][PF ₆]	25		38-52	<i>H</i> ₁		108
				[BMIM][PF ₆]	25		65-87	<i>L</i> _α		
					25		45		lattice-spacing = 12.30 ^e	108
					25		50		lattice-spacing = 11.97 ^e	
					25		68		lattice-spacing = 10.82 ^e	
					25		75		lattice-spacing = 10.50 ^e	
					25		85		lattice-spacing = 10.00 ^e	
					25		40	<i>H</i> ₁	d-spacing ≈ 12 ^e	51
					25		50	<i>H</i> ₁ + <i>L</i> _α	d-spacing ≈ 11.5 ^e	
					25		60	<i>H</i> ₁ + <i>L</i> _α	d-spacing ≈ 11.3 ^e	
					25		70	<i>L</i> _α	d-spacing ≈ 11 ^e	
					25		80	<i>L</i> _α	d-spacing ≈ 10 ^e	
					25		85	<i>L</i> _α	d-spacing ≈ 9.8 ^e	
				EAN	25		~30	<i>I</i> ₁		109
					25		44-64	<i>H</i> ₁		
					25		66-90	<i>L</i> _α		
					25		92-94	<i>V</i> ₂		
					25		45		lattice-spacing = 13.10 ^e	
					25		50		lattice-spacing = 12.80 ^e	
					25		68		lattice-spacing = 11.51 ^e	
					25		75		lattice-spacing = 11.18 ^e	
					25		85		lattice-spacing = 10.59 ^e	
5		PS-P2VP		[Im][TFSI]	145	3		<i>L</i> _α , cylindrical, disordered phases	d-spacing = 23.7	105
					225	3			d-spacing = 23	

- The self-assembled morphologies are denoted as: *I*₁ = normal micellar cubic phase, *H*₁ = normal hexagonal phase, *L*_α = lamellar phase, *V*₂ = reverse bicontinuous cubic phase.

Ion gels

ILs possess several traits, such as electro-mechanical stability and high ion conductivity, which make them excellent candidates as electrolyte materials. However, many applications or devices require a solid electrolyte materials rather than a liquid electrolyte. Incorporating ILs into solid or quasi-solid microstructures provided by self-assembled ABCs can lead to the formation of solid ABC/IL binary composite materials, referred to as “ion gels”. Systems where ILs are solidified (or gelled) by polymers are soft solids with significant ion conductivity often comparable to that of neat ILs.^{80,136} Here again, formulating ion gels for specific applications will benefit from robust structure-property relationship for both the quiescent state and under deformations. This section provides a brief overview on the emerging body of research on ion gels comprised of non-ionic ABC in ILs. Space limitations prevent us from reviewing work on other polymer/IL electrolyte materials⁷ and their electrochemical applications as well as corresponding factors affecting ion transport.⁸

Microstructure-electrical property relationship of ion gels in quiescent state

Four categories of ABC/IL ion gels can be identified based primarily on their synthetic route. First, blending ILs with polymers can produce ion gels. The typical preparation methods for preparing ion gel membranes are self-assembly with solvent casting, or hot-pressing. Ion gels synthesized using this method are mostly reported for application in lithium batteries. It is proposed that the ideal polymer for ion gel electrolyte design should limit the interaction of the charged transport species with the polymer backbone and often incorporate a hydrophobic plasticizer.¹³⁷ Typical polymers reported are PEO homopolymer¹³⁸⁻¹⁴⁰ and PVdF-PHP^{137,141-143} diblock copolymer (Table 3). Although Park *et al.* has recently reviewed this topic for lithium battery application,⁸ it is note-worthy to pointing out that the ion conductivity for these self-assembled ion gels are usually fall within the range of 10^{-5} - 10^{-2} S/cm at room temperature. Equally importantly, however, the mechanical properties vary vastly ranges from brittle to flexible behavior based on the specific choice of polymers and ILs.

While the conductivities of ILs increase with increasing IL concentration, the mechanical properties of the membranes tend to weaken with increasing IL concentration using the first synthetic route.^{99,144} One way to boost mechanical properties while largely maintaining high conductivity is to chemically cross link polymer network with ILs, which is the second synthetic route. Chemically cross-linked ion gels can be prepared via free radical polymerization of vinyl monomers in the presence of a cross-linking agent¹⁴⁵⁻¹⁴⁷ or via polyaddition reaction of macromonomers with functionalized reactive groups.¹⁴⁸⁻¹⁵¹ In the first report of cross-linked ion gel containing PMMA in [EMIM]TfSA using ethylene glycol dimethacrylate as a cross-linker,¹⁴⁵ the ionic conductivity of the ion gels reaching almost 6 mS/cm at the lower polymer concentration, and the storage modulus was found to be on the order of 0.1 GPa for gel with 80 mol% PMMA. Interestingly, an unexpected finding of more free charge carriers in the ion gel than in the neat IL at certain compositions was reported. It was proposed that the increased ion dissociation resulted from specific interactions between the PMMA matrix and the IL ions. Although this method was found to be fairly robust, and yielded good ion conductivity in the order of 10^{-2} S/cm at room temperature, little of the mechanical properties on binary ABC based ion gels were reported.

The third synthetic route is physical cross-linking. ABCs are especially versatile candidates in this synthetic route, because they provide more flexibility in controlling the gel structure and properties through variations of block length/composition/sequence, ABC concentration, and the choice of monomer units. Physically cross-linked ion gel could be synthesized through the gelation of ABA type triblock copolymers with IL incompatible A blocks and an IL compatible B block in ILs. Specific examples include PS-PEO-PS and PS-PMMA-PS⁸⁰⁻⁸² triblock copolymers in AILs with alkyl imidazolium cations and varying anions. The ABA type triblock copolymers composed of short, hard A blocks and long, soft B blocks are typically thermoplastic elastomers. The underlying principle of physically cross-linking ion gels lies in the selective solvation of ILs towards different polymer blocks. To explain this in more details, when an ABA triblock copolymer dissolves in IL, where IL is selective to B blocks but not A block, then a core-shell micelle with

A in the core and B in the shell will form. At sufficient high enough concentration, ABA polymer chains will act as cross-linking points and bridge between micelles resulting in polymer network. In He *et al.*'s study of physically cross-linked PS-PEO-PS in [BMIM][PF₆], ion gels were formed with as little as 5 wt% copolymer, and the ionic conductivity was closed to that of neat IL.⁸⁰ With a series of systematic studies on physically cross-linked ABA triblock copolymer/AIL ion gels, Zhang *et al.* generalize the material design rules.⁸¹ To achieve a higher modulus, the rule suggests that more polymer should be added or using a midblock with a smaller entanglement molecular weight. Once the midblock is chosen, to minimize the loss in conductivity, PS end-blocks should be relatively short but long enough to obtain a persistent gel with high enough mechanical integrity at desired temperature. Using the physically cross-linking route, the resulting ion gels have high conductivity that is comparable to the neat IL, thermal stability, sufficient mechanical strength, and a narrower distribution of the mesh size in the polymer network. As mentioned earlier, this method is promising because of its advantages in controllability and tunability in its components (polymer or ILs) and the physical reversibility of the cross-linking, which can aid in processing. More importantly, in comparison to 10-30 wt % of polymers in conventional polymer gels, much less polymer is required to form an ion gel using triblock copolymers, which can improve the ionic conductivity. Of noteworthy interest, the application of physically cross-linking method with thermos-sensitive diblock copolymer, such as previously reviewed UCST phase behavior of PNIPAm in [EMI][TFSI] and LCST phase behavior of PNIPAm/water, can produce thermos-responsive ion gels.⁸³

The fourth method to produce ion gels with enhanced mechanical properties is to combine the self-assembly provided by ABCs with subsequent chemical cross-linking steps.^{136,152} This synthetic route takes advantages of both chemical and physical cross-linking routes, i.e. the conductivity can be tuned for a specific application by manipulating the self-assembled microstructure, while the enhanced mechanical strength for the solid electrolyte can be achieved by subsequent cross-linking step. Gu *et al.* reported the synthesis of ion gels by self-assembly of PS-PEO-PS, of which 25% of the styrene units have a pendant azide functionality, in [EMIM][TFSI], followed by chemical cross-linking of the azide groups by thermal annealing.¹⁵² The latter step provides enhanced mechanical toughness to the ion gel without significant detriment on its ionic conductivity. Similarly, Miranda and co-workers synthesized PPO-PEO-PPO with crosslinkable end groups.¹³⁶ By self-assembly in [BMIM][PF₆] and subsequent photo-cross-linking, highly conductive, solid, elastic gels was produced. López-Barrón and colleagues recently reported the synthesis of ultra-stretchable soft iono-elastomers by sequential self-assembly of inexpensive, commercially available PEO-PPO-PEO (Pluronic F127) with acrylated end groups in d₃EAN and subsequent photo-crosslinking the resulted micellar FCC lattices.⁶⁸ These materials provide a combination of high conductivity, remarkable stretchability, tensile properties and mechano-electrical response,¹⁵³ which will be detailed reviewed in the next section. To summarize, cross-linking of these polymers through their end groups was sufficient to impart mechanical stability to the gels, which did not have a significant effect on the conductivity or the microstructure of the gels.

Microstructure-property relationships of ion gel under deformation

Ion gels with high conductivity and high stretchability are becoming an important area of research due to emerging technologies involving stretchable electronics.¹⁵⁴ However, the work in this field is much less developed due to the complexity in sample preparation, manufacturing processes and characterization tools.

As reviewed in the previous section, the solid ion gels prepared by Gu and coworkers exhibited strain-to-break values of ~350%.¹⁵² López-Barrón *et al.* detailed investigated the relationship among microstructure, tensile properties and mechano-electrical responses under uniaxial deformation for synthesized Pluronic 127DA/d₃EAN ion gels.¹⁵³ In tensile property measurement, remarkably large values of both strain to break and tensile strength were measured (Table 4) as illustrated in Figure 6(a). During uniaxial extension, shown in Figure 6(b), a pronounced Mullins effect was observed, which is a typical response of elastomer composites.¹⁵³ The mechano-electrical response of the iono-elastomer in Figure 6(c) reveals a very surprising and counterintuitive response, namely, the resistance decreases with strain, which indicates that the intrinsic conductivity of the material increases during the stretching process. *In situ* small

angle X-ray (SAXS) measurements show this to be a consequence of a strain-induced micro-structural rearrangement. Figure 6d shows the in-situ SAXS measurements, where the microstructural origin of the unique mechano-electrical response during uniaxial deformation was elucidated to be a reversible extensional strain-induced FCC-to-HCP transition. It was hypothesized that this transition is responsible for the conductivity increase during stretching, and further, that its reversibility is due to complex network structure formed during crosslinking of micellar FCC lattice.⁶⁸

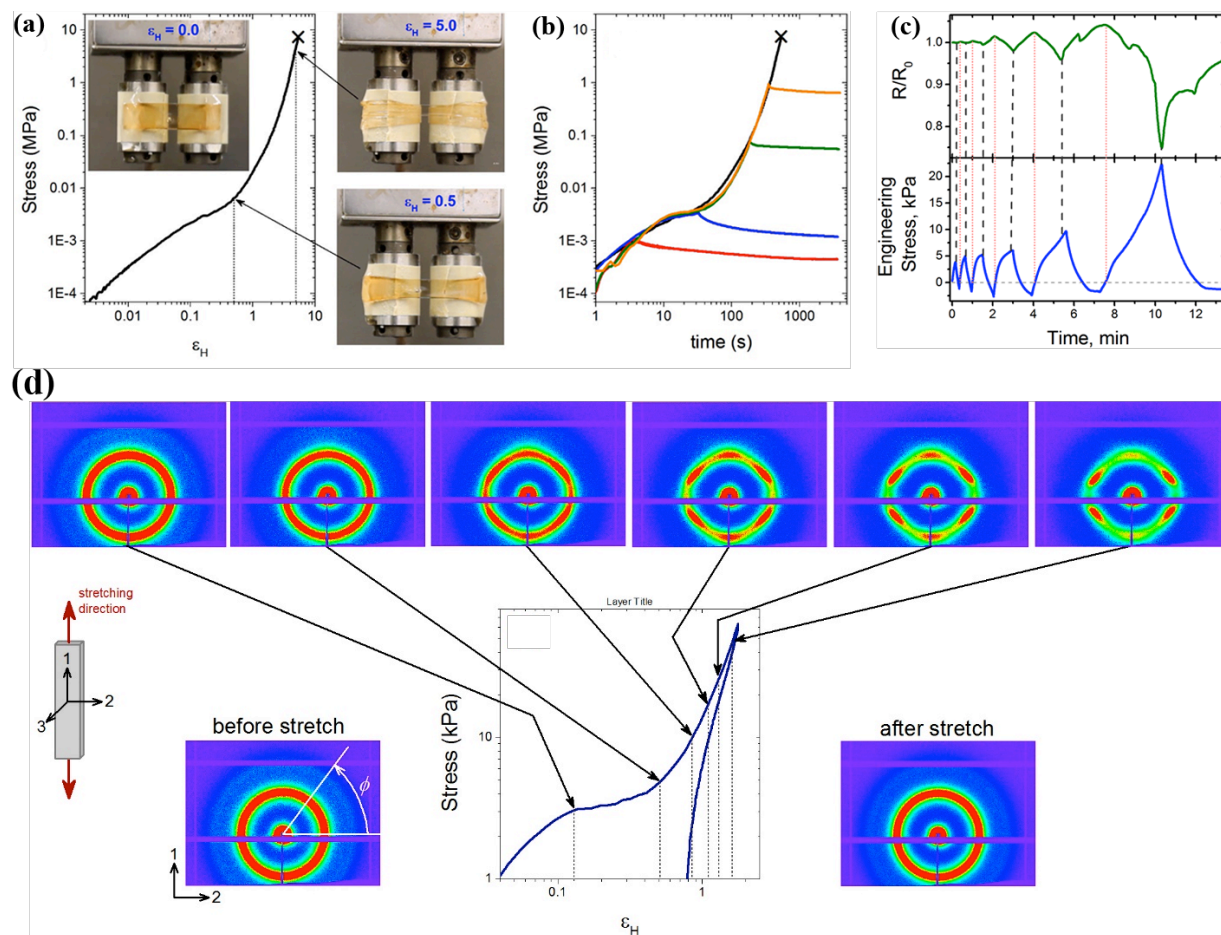


Figure 6: Tensile properties of crosslinked 24 wt% F127-DA/dEAN solution. (a) Stress-strain curve measured in the SER (with Hencky strain rate = 0.01 s⁻¹). The photographs show the sample being stretched at the indicated Hencky strains. (b) Stress (measured in the SER, with Hencky strain rate = 0.01 s⁻¹) as a function of time showing loading to Hencky strains of 0.032, 0.32, 2 and 4, followed by relaxation for 1 hr. (c) Electro-mechanical hysteresis tests. Normalized electrical resistance and stress as a function of time during hysteresis tests. (d) In-situ SAXS measurements during uniaxial deformation. Stress-strain curve measured in the Linkam tensile stage, and 2D SAXS profiles measured at the strain values indicated by the arrows. Also shown are the 2D SAXS profiles measured before and after loading.¹⁵³

Summary and outlook

Ion gels composed of non-ionic ABCs and ILs are a growing topic of research because of their potential for such applications as membranes for batteries and stretchable electronics. ABC-based ion gels have the versatility and tunability for designing the mechanical scaffold for supporting ion transport of the incorporated ILs. Here, we briefly summarize four synthetic routes and point out their advantages and disadvantages to aid in designing systems for specific applications. However, the challenges remain for effective formulation. On the one hand, general rules for balancing the trade-off between mechanical and

electrical properties are not yet established. Although, in general, the addition of polymer and or crosslinking into ion gels increases the mechanical integrity and lowers the ionic conductivity, specific ion-polymer interactions, and as shown, self-organized microstructures, must be considered in formulation. With the nearly unbounded number of possible ion gel compositions possible, generalized guidelines for predicting the microstructural-mechanical-electrical property relationships for ion gels at rest and under deformation would be tremendously valuable for designing ion gels for specific applications. In particular, quantification of ion transport in ion gels especially is poorly understood. Park *et al.* provide a review on the diverse factors affecting the ion transport properties in polymer/IL electrolytes for lithium batteries, fuel cells and electro-active actuators,⁸ such systematic examinations are warranted for other applications of ion gels.

Table 4: Examples of block copolymers containing ionic liquids: block copolymers, ion liquids, block copolymer contents and proton conductivities.

Line	Block copolymer	Ionic liquid	Synthesis pathway	Cross-linking agent	BC/IL/CL (wt%)	Measured temp (°C)	Stress to break	Conductivity (mS/cm)			Ref		
								Neat IL	Un-crosslinked	Cross-linked			
1	PVdF-PHFP	[EMIM][Trif]	Hot pressing with PC, then freeze drying off PC		48/52	~22				1.1		141	
			50/50		1.3								
		33/67	5.6										
		50/50	1.8										
		[EMIM][BF ₄]	Hot pressing with PC, then freeze drying off PC	71/29					0.1				
	Hot pressing without cosolvent		16/84				8.0						
			Hot pressing without cosolvent	9/91					7.3				
			Hot pressing without cosolvent	33/67					5.8				
				13/87					11.0				
2	Pluronic 25R4	[BMIM][PF ₆]	Self-assembly ^a		20/80	25			≈1.49	0.61	0.61	136	
3	Pluronic 64R4				50/50					0.24			0.14
4	Pluronic 45R6				20/80					0.76			0.83
					50/50					0.37			0.31
		10/90	1.24	1.22									
		20/80	0.79	0.76									
		50/50	0.25	0.22									
5	Pluronic 45R6		Subsequential self-assembly and chemical cross-linking ^b	PPO-acrylate	10/90/05					0.93	0.98		
					20/80/10					0.68	0.64		
					20/80/10					0.60	0.35		
6	PS-PEO-PS	[BMIM][PF ₆]	Self-assembly with cosolvent CH ₂ Cl ₂ ^a		1/99	26.5		1.62	1.6			80	
					3/97	26.5		1.62	1.55				
					5/95	26.5, 80		1.62, 15	1.47, 13				
					7/93	26.5		1.62	1.32				
					10/90	26.5, 80		1.62, 15	1.12, 11				
7	PS-PEO-PS	[EMIM][TFSA]	Self-assembly with cosolvent CH ₂ Cl ₂ ^a		10/90	25, 80				6.1, 22		81	
					40/60	60, 160				3.5, 18			
					50/50	60, 160				2.4, 12			
8	PS-PEO-PS	[EMIM][TFSA]	Self-assembly with cosolvent CH ₂ Cl ₂ ^a		10/90	40	≈0.75x10 ⁵	≈12		≈9.2		152	
9	PS-PEO-PS with azide functional end groups		Subsequential self-assembly and chemical cross-linking at elevated temperature or UV irradiation ^b		10/90	40	≈3.6x10 ⁵			≈9.1	≈8.9		
10	PS-PMMA-PS	[EMIM][TFSA]	Self-assembly with cosolvent CH ₂ Cl ₂ ^a		10/90	25				5.5		81	
					30/70	40, 200				0.85, 18			
					40/60	40, 200				0.32, 12			
					50/50	40, 200				0.071, 7.1			
11	PNIPAm-PEO-PNIPAm	[EMIM][TFSI]	Self-assembly ^a		10/90	20		8	4			83	
12	Pluronic F127	d ₃ EAN	Self-assembly ^a		15/85	20			25.7	10.8	11.0	68	
						40			35.4	25.3	25.9		
						60			41.6	37.0	36.9		
					22.5/77.5	20			25.7	10.8	12.0		
						40			35.4	21.5	23.7		
						60			41.6	35.7	39.1		

13	Pluronic F127 with acrylate functional end groups	d ₃ EAN	Subsequential self-assembly and chemical cross-linking by UV irradiation ^b	1-hydroxycyclohexyl phenyl ketone	24/76/1	25	4.7±0.8 MPa	28		15	153
----	---	--------------------	---	-----------------------------------	---------	----	-------------	----	--	----	-----

- The type of ion gels form are ^aphysical ion gel, ^bchemically cross-linked ion gel, ^cthin film.
- BC/IL/CL indicates Block copolymer/Ionic liquid/Cross-linker.

Emerging applications of block copolymer self-assembly in ionic liquids

Electrochemical applications and devices

Self-assembly of ABCs in ILs is of technological interest for electrochemical applications or as electrolytes in next-generation electrochemical devices,⁸ including lithium ion batteries,¹⁵⁵ solar cells,¹⁵⁶ electro-mechanical actuators^{157,158} and electrolyte-gated transistors,^{159,160} and light-emitting electrochemical cells, in which microphase-separated ABCs enable the optimization of disparate properties such as mechanical stability and ion transport or light emission. As demonstrated in the previous sections and summarized in Table 5, block copolymers containing a PEO block or side-chain, a PMMA block, or a P2VP block have been frequently used as model systems in such studies due to the ability of the ether, acrylate, and pyridine chemistries to solvate a wide variety of ions.⁸⁴ ABCs provide flexibility in tuning micelle size and nanostructure during self-assembly, yet their noncovalently-bounded structures may require further stabilization for those applications. One approach is to use highly amphiphilic block copolymers to obtain deeply metastable micelle structures by making extremely low CMC.^{27,161,162} This reduces the probability of demicellization via changing external factors such as temperature, pH, and solvent quality. Another method is to covalent cross-linking the core¹⁶³ or the shell,¹⁶⁴⁻¹⁶⁶ which will lead to the formation of ion gel in ILs with enhanced mechanical strength and greater stability as discussed earlier.⁸⁴

Nano delivery vehicles

Block copolymer micelles and vesicles have received considerable attention for their ability to encapsulate, transport, and deliver small molecules or solvents in harsh environment. With the exploration of ILs as self-assembly media, block copolymer micelles and vesicles have been extensively investigated for potential as delivery vehicles, especially in the field of catalyst nanoreactors,¹⁶⁷ drug delivery¹⁶⁸ and phase transfer.⁸⁵ However, further advancing in these technologies requires not only finding new ABC/IL systems, but also understanding the interaction between the carriers and interior capsule, and the carrier and exterior environment are pivotal. For example, the relationship between nanoreactor microstructure and catalyst properties in ILs have rarely been explored in polymeric nanoreactors. Developing these relationships requires detailed *in situ* characterization of the nanoscale structure and a deep fundamental understanding of the factors that govern the structure and dynamics of macromolecular assemblies.²⁹ In the case of drug delivery, efficacy requires a systematic understanding of the vehicle structure, surface functionality, reactions between drug and vehicle, drug-loading/release procedures and solution processing conditions.

Wearable electronics and sensors and smart textiles

Self-assembly of ABCs in ILs can form aforementioned subset of ion gels (iono-elastomers), which are candidates for use in emerging technologies involving stretchable electronics, with potential applications as stretchable batteries,¹⁶⁹ wearable sensors¹⁷⁰ and integrated circuits.^{171,172} In principle, wearable electronics and sensors can be woven into clothing, uniforms, and sporting equipment to create smart textiles¹⁷³ and some applications are shown in Figure 7.¹⁵⁴

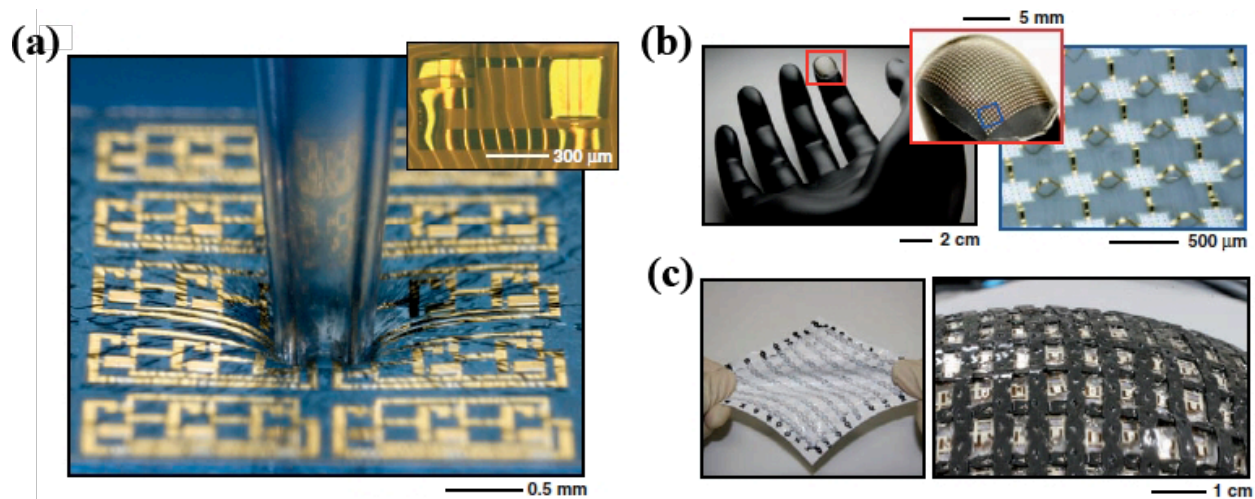


Figure 7: Examples of stretchable electronics. (a) Stretchable silicon circuit in a wavy geometry, compressed in its center by a glass capillary tube (main) and wavy logic gate built with two transistors (top right inset). (b) Stretchable silicon circuit with a mesh design, wrapped onto a model of a fingertip, shown at low (left), moderate (center) and high (right) magnification. The red (left) and blue (center) boxes indicate the regions of magnified views in the center and right, respectively. The image on the right was collected with an automated camera system that combines images at different focal depths to achieve a large depth of field. (c) Array of organic transistors interconnected by elastic conductors on a sheet of PDMS in a stretched (left) and curvilinear (right) configuration. The figure was reproduced from ¹⁵⁴. Reprinted with permission from ¹⁵⁴. Copyright © 2010, American Association for the Advancement of Science.

Table 5: Examples of representative block copolymers/ionic liquids system for various application.

Line	Applications	Representative ABCs	Representative IL cations	Working principle
1	Lithium batteries	PEO-based polymer: PS-PEO, PEO-PMMA ¹⁷⁴ PVdF-PHFP	AILs composed of alkyl pyrrolidinium, alkyl imidazolium, and alkyl sulfonium cations and anions can vary.	ILs can act as a plasticizer to accelerate relaxation of polymer chains, i.e., the lowering of the glass transition temperature (T_g) of the polymers.
2	Fuel cell	Nafion TM PBI PVdF-HFP PMMA (and PMMA based copolymers) P2VP (and P2VP based copolymers) PSS (and PSS based copolymers)	AILs comprise heterocyclic diazolum or alkylimidazolium with short alkyl chains cations, and anions can vary.	Incorporation of nonvolatile and highly conductive ILs into polymer matrices is a facile means to obtain high conductivity under water-free conditions and high temperatures.
3	Electro-active actuators	PVdF-PHFP Nafion TM		Incorporating IL into ionic polymer layer of the actuator can improve the performance, by reducing Young's modulus, facilitating ion transport, and enhancing electrochemical stability
4	Nanoreactor	Bi or tri block ABCs that can form micelles or vesicles in ILs.	Both AILs and PILs.	ABCs can self-assemble into micelles or vesicles in ILs, which can be used as nano delivery vehicles.
5	Wearable electronics	Triblock copolymers: PS-PEO-PS, PPO-PEO-PPO, PEO-PPO-PEO	AILs with alkyl imidazolium cations and anions can vary. PIL reported is d ₃ EAN.	Iono-elastomers composed of self-assembled ABCs in ILs possess ultra-strechability and high ion conductivity can be used for wearable electronics application.

Conclusion and outlooks

An overview of the field reveals a remarkable breadth of possible microstructure and properties that can result from the self-assembly of block copolymers in ILs. In the quiescent state, the self-assembly of block copolymers in ILs is often compared to that in aqueous solutions. Under flow condition, *in situ* SANS and SAXS combining with rheology and dielectric measurements provides critical and unique spatiotemporal resolved structural information on length scales of direct relevance to the macroscopic properties for various applications. Work to date spans interests in both fundamental investigations and technical applications of block copolymer self-assembly in ionic liquids, but the wealth of possible chemistries and ability to create a plethora of hierarchically self-assembled microstructures suggests that many new discoveries await.

To further the successful application of block copolymer/IL applications, a number of challenges should be addressed. Materials genomic approaches may prove to be particularly valuable given the effectively infinite range of possible chemistries. A priori predictions of ion-polymer interactions and guidelines for selecting polymer architectures to promote specific microstructures would greatly accelerate materials design and development. Further, as ILs are often highly hygroscopic, and the self-assembly of ABCs in ILs are often time consuming and path dependent, consistent and reproducible sample preparation and processing must be established. Here, advances in micro- and nano- scale probes, and precision tools for measuring the rheological, mechanical, and electrical properties of microscopic quantities of samples to determine connections between properties and processing conditions is critical in the development of characterization techniques. Such property relationships will unequivocally require measurements of nano and mesoscale microstructure. Recent advances in instrumentation, such as the dielectric-rheo-SANS sample environment¹⁷⁵ could accelerate materials development. Meanwhile, direct visualization of self-assembled microstructure using TEM has been proved to be useful (references) but still limited by contrast and to thin samples. More reliable and applicable direct imaging techniques would be significantly beneficial to the field. Lastly, even though commercially available ABCs have been incorporated into ILs, the mass fabrication of devices will require considerations of product lifecycle and follow principles of green engineering. Specifically, low-cost ILs with human and environmental compatibility would be valuable. The rapid growth in developments in the self-assembly of ABCs in ILs promises to create hierarchically functional materials with technologically useful emergent properties. The field is inherently multi-disciplinary and these materials promise solutions across a broad range of technological needs.

Appendix

Acronym	Chemical name
[BMIM][BF ₄]	1-butyl-3-methylimidazolium tetrafluoroborate
[BMIM][FAP]	1-butyl-3-methylimidazolium tris(pentafluoroethyl)trifluorophosphate
[BMIM][PF ₆]	1-butyl-3-methylimidazolium hexafluorophosphate
CH ₂ Cl ₂	methylene chloride
EAN	ethylammonium nitrate
d ₃ EAN	Partially deuterated ethylammonium nitrate
[EMIM][BF ₄]	1-ethyl-3-methylimidazolium tetrafluoroborate
[EMIM][NfF ₂]	1-ethyl-3-methylimidazolium bis(trifluoromethane sulfonyl)imide
[EMIM][TFSA]	1-ethyl-3-methylimidazolium bis-(trifluoromethylsulfonyl)amide
[EMIM][TFSI]	1-ethyl-3-methylimidazolium bis(trifluoromethylsulfonyl)imide
[EMIM][Trif]	1-ethyl-3-methylimidazolium triflate
[Im][TFSI]	Imidazolium bis(trifluoromethane)sulfonamide
P2VP	Poly(2-vinylpyridine)
PAN	penthylammonium nitrate

PB-PEO	Poly(butadiene-b-ethylene oxide)
PBI	Polybenzimidazole
PBnMA-PMMA	Poly(benzyl methacrylate-b-methyl methacrylate)
PEGE-PEO	Poly(ethyl glycidyl ether-b-ethylene oxide)
PEO-PNIPAm	Poly(ethylene oxide-b-N-isopropylacrylamide)
PEO-b-P(AzoMA-r-NIPAm)	Poly(ethylene oxide-b(4-phenylazophenyl methacrylate-r- N-isopropylacrylamide))
PEO-PPO-PEO	Poly(ethylene oxide-b-propylene oxide-b-ethylene oxide)
PGPrE-PEO	Poly(glycidyl propyl ether- b-ethylene oxide)
PnBMA-PEO	poly(n-butyl methacrylate-b-ethylene oxide)
PnBMA-PMMA	poly(n-butyl methacrylate-b-methyl methacrylate)
PS-P2VP	Poly(styrene-b-2-vinylpyridine)
PS-PEO	poly(styrene-b-ethylene oxide)
PS-PMMA	poly(styrene-b-methyl methacrylate)
PS-PEO-PS	poly(styrene-b-ethylene oxide-b-styrene)
PS-PMMA-PS	poly(styrene-b-methyl methacrylate-b-styrene)
PSS	Poly(styrenesulfonate)
PNIPA, PNIPAAm, NIPA, PNIPAA or PNIPAm	Poly(N-isopropylacrylamide)
PPO-PEO-PPO	Poly(propylene oxide-b-ethylene oxide-b-propylene oxide)
PVdF-PHFP	poly(vinylidene fluoride-b-hexafluoropropylene)

Acknowledgements

The authors acknowledge the support of the National Institute of Standards and Technology (NIST), U.S. Department of Commerce, in providing the neutron research facilities used in this work. N.J.W. and R.C. acknowledge the support of cooperative agreements 70NANB12H239 and 70NANB15H260 from NIST. The statements, findings, conclusions, and recommendations are those of the authors and do not necessarily reflect the views of NIST or the US Department of Commerce. R.C. acknowledges support from the National Science Foundation Graduate Research Fellowship under Grant No.1247394.

References

- (1) Riess, G. Micellization of Block Copolymers. *Prog. Polym. Sci.* **2003**, *28*, 1107–1170.
- (2) Hayes, R.; Warr, G. G.; Atkin, R. Structure and Nanostructure in Ionic Liquids. *Chem. Rev.* **2015**, *115*, 6357–6426.
- (3) Greaves, T. L.; Drummond, C. J. Protic Ionic Liquids: Evolving Structure-Property Relationships and Expanding Applications. *Chem. Rev.* **2015**, *115*, 11379–11448.
- (4) Greaves, T. L.; Drummond, C. J. Ionic Liquids as Amphiphile Self-Assembly Media. *Chem. Soc. Rev.* **2008**, *37*, 1709–1726.
- (5) Greaves, T. L.; Drummond, C. J. Solvent Nanostructure, the Solvophobic Effect and Amphiphile Self-Assembly in Ionic Liquids. *Chem. Soc. Rev.* **2013**, *42*, 1096–1120.
- (6) Ueki, T.; Watanabe, M. Polymers in Ionic Liquids: Dawn of Neoteric Solvents and Innovative Materials. *Bull. Chem. Soc. Jpn.* **2012**, *85*, 33–50.
- (7) Ye, Y. S.; Rick, J.; Hwang, B. J. Ionic Liquid Polymer Electrolytes. *J. Mater. Chem. A* **2013**, *1*, 2719–2743.
- (8) Park, M. J.; Choi, I.; Hong, J.; Kim, O. Polymer Electrolytes Integrated with Ionic Liquids for Future Electrochemical Devices. *J. Appl. Polym. Sci.* **2013**, 2363–2376.
- (9) Hamley, I. W. *The Physics of Block Copolymers*; Oxford University Press: New York, NY, 1998.
- (10) Lindman, B.; Alexandridis, P. *Amphiphilic Block Copolymers : Self-Assembly and Applications*;

- Elsevier: Amsterdam ; New York, 2000.
- (11) Hamley, I. W. *Block Copolymers in Solution : Fundamentals and Applications*; Wiley: Chichester, England ; Hoboken, NJ, 2005.
 - (12) Weingärtner, H. Understanding Ionic Liquids at the Molecular Level: Facts, Problems, and Controversies. *Angew. Chem. Int. Ed.* **2008**, *47*, 654–670.
 - (13) Atkin, R.; Warr, G. G. Structure in Confined Room-Temperature Ionic Liquids. *J. Phys. Chem. C* **2007**, *111*, 5162–5168.
 - (14) Atkin, R.; Warr, G. G. The Smallest Amphiphiles: Nanostructure in Protic Room-Temperature Ionic Liquids with Short Alkyl Groups. *J. Phys. Chem. B* **2008**, *112*, 4164–4166.
 - (15) Hayes, R.; Warr, G. G.; Atkin, R. At the Interface: Solvation and Designing Ionic Liquids. *Phys. Chem. Chem. Phys.* **2010**, *12*, 1709–1723.
 - (16) Hayes, R.; Imberti, S.; Warr, G. G.; Atkin, R. Amphiphilicity Determines Nanostructure in Protic Ionic Liquids. *Phys. Chem. Chem. Phys.* **2011**, *13*, 3237–3247.
 - (17) Hayes, R.; Imberti, S.; Warr, G. G.; Atkin, R. Effect of Cation Alkyl Chain Length and Anion Type on Protic Ionic Liquid Nanostructure. *J. Phys. Chem. C* **2014**, *118*, 13998–14008.
 - (18) Gao, J.; Wagner, N. J. Water Nanocluster Formation in the Ionic Liquid 1-Butyl-3-Methylimidazolium Tetrafluoroborate ([C4mim][BF4])-D2O Mixtures. *Langmuir* **2016**, *32*, 5078–5084.
 - (19) López-Barrón, C. R.; Li, D.; Derita, L.; Basavaraj, M. G.; Wagner, N. J. Spontaneous Thermoreversible Formation of Cationic Vesicles in a Protic Ionic Liquid. *J. Am. Chem. Soc.* **2012**, *134*, 20728–20732.
 - (20) Israelachvili, J. N. *Intermolecular and Surface Forces*; Academic Press: Burlington, MA, 2011.
 - (21) Considine, R. F.; Drummond, C. J. Long-Range Force of Attraction between Solvophobic Surfaces in Water and Organic Liquids Containing Dissolved Air. *Langmuir* **2000**, *16*, 631–635.
 - (22) Alexandridis, P.; Alan Hatton, T. Poly(ethylene Oxide)-Poly(propylene Oxide)-Poly(ethylene Oxide) Block Copolymer Surfactants in Aqueous Solutions and at Interfaces: Thermodynamics, Structure, Dynamics, and Modeling. *Colloids Surf., A.* **1995**, *96*, 1–46.
 - (23) Halperin, A.; Tirrell, M.; Lodge, T. P. Tethered Chains in Polymer Microstructures. *Adv. Polym. Sci.* **1992**, *100*, 31–71.
 - (24) Hayes, R.; Imberti, S.; Warr, G. G.; Atkin, R. The Nature of Hydrogen Bonding in Protic Ionic Liquids. *Angew. Chem. Int. Ed.* **2013**, *52*, 4623–4627.
 - (25) Jain, S. On the Origins of Morphological Complexity in Block Copolymer Surfactants. *Science*. **2003**, *300*, 460–464.
 - (26) Lund, R. Small Angle Neutron Scattering as a Tool to Study Kinetics of Block Copolymer Micelles. In *Studying Kinetics with Neutrons : prospects for time resolved neutron scattering*; Springer Series in Solid-State Sciences 161; Springer: Berlin : New York, 2009; pp 213–240.
 - (27) Won, Y. Y.; Davis, H. T.; Bates, F. S. Molecular Exchange in PEO–PB Micelles in Water. *Macromolecules* **2003**, *36*, 953–955.
 - (28) Hayward, R. C.; Pochan, D. J. Tailored Assemblies of Block Copolymers in Solution: It Is All about the Process. *Macromolecules* **2010**, *43*, 3577–3584.
 - (29) Kelley, E. G. Synthesis, Solution Assembly, and Characterization of Amphiphilic Block Polymers. Ph.D. Dissertation, University of Delaware, Newark, DE, 2014.
 - (30) Choi, S. H.; Lodge, T. P.; Bates, F. S. Mechanism of Molecular Exchange in Diblock Copolymer Micelles: Hypersensitivity to Core Chain Length. *Phys. Rev. Lett.* **2010**, *104*, 47802.
 - (31) Mok, M. M.; Thiagarajan, R.; Flores, M.; Morse, D. C.; Lodge, T. P. Apparent Critical Micelle Concentrations in Block Copolymer/ionic Liquid Solutions: Remarkably Weak Dependence on Solvophobic Block Molecular Weight. *Macromolecules* **2012**, *45*, 4818–4829.
 - (32) Kelley, E. G.; Murphy, R. P.; Seppala, J. E.; Smart, T. P.; Hann, S. D.; Sullivan, M. O.; Epps, T. H. Size Evolution of Highly Amphiphilic Macromolecular Solution Assemblies via a Distinct Bimodal Pathway. *Nat. Commun.* **2014**, *5*, 3599.
 - (33) Halperin, A.; Alexander, S. Polymeric Micelles: Their Relaxation Kinetics. *Macromolecules* **1989**,

- 22, 2403–2412.
- (34) Esselink, F. J.; Dormidontova, E.; Hadziioannou, G. Evolution of Block Copolymer Micellar Size and Structure Evidenced with Cryo Electron Microscopy. *Macromolecules* **1998**, *31*, 2925–2932.
 - (35) Esselink, F.; Dormidontova, E.; Hadziioannou, G. Redistribution of Block Copolymer Chains between Mixed Micelles in Solution. *Macromolecules* **1998**, *31*, 4873–4878.
 - (36) Li, Z.; Dormidontova, E. E. Kinetics of Diblock Copolymer Micellization by Dissipative Particle Dynamics. *Macromolecules* **2010**, *43*, 3521–3531.
 - (37) Li, Z.; Dormidontova, E. E. Equilibrium Chain Exchange Kinetics in Block Copolymer Micelle Solutions by Dissipative Particle Dynamics Simulations. *Soft Matter* **2011**, *7*, 4179–4188.
 - (38) Evans, D. F.; Yamauchi, A.; Roman, R.; Casassa, E. Z. Micelle Formation in Ethylammonium Nitrate, a Low-Melting Fused Salt. *J. Colloid Interface Sci.* **1982**, *88*, 89–96.
 - (39) Evans, D. F.; Yamauchi, A.; Wei, G. J.; Bloomfield, A. Micelle Size in Ethylammonium Nitrate As Determined by Classical and Quasi-Elastic Light Scattering. *J. Phys. Chem.* **1983**, *87*, 3537–3541.
 - (40) Ueki, T.; Arai, A. A.; Kodama, K.; Kaino, S.; Takada, N.; Morita, T.; Nishikawa, K.; Watanabe, M. Thermodynamic Study on Phase Transitions of Poly(benzyl Methacrylate) in Ionic Liquid Solvents. *Pure Appl. Chem.* **2009**, *81*, 1829–1841.
 - (41) Evans, D. F.; Kaler, E. W.; Benton, W. J. Liquid Crystals in a Fused Salt: B, γ -Distearoylphosphatidylcholine in N-Ethylammonium Nitrate. *J. Phys. Chem.* **1983**, *87*, 533–535.
 - (42) Araos, M. U.; Warr, G. G. Self-Assembly of Nonionic Surfactants into Lyotropic Liquid Crystals in Ethylammonium Nitrate, a Room-Temperature Ionic Liquid. *J. Phys. Chem. B* **2005**, *109*, 14275–14277.
 - (43) Bordel Velasco, S.; Turmine, M.; Di Caprio, D.; Letellier, P. Micelle Formation in Ethyl-Ammonium Nitrate (an Ionic Liquid). *Colloids Surfaces A Physicochem. Eng. Asp.* **2006**, *275*, 50–54.
 - (44) Batrakova, E.; Lee, S.; Li, S.; Venne, A.; Alakhov, V.; Kabanov, A. Fundamental Relationships between the Composition of Pluronic Block Copolymers and Their Hypersensitization Effect in MDR Cancer Cells. *Pharm. Res.* **1999**, *16*, 1373–1379.
 - (45) Alexandridis, P.; Holzwarth, J. F.; Hatton, T. A. Micellization of Poly(ethylene Oxide)-Poly(propylene Oxide)-Poly(ethylene Oxide) Triblock Copolymers in Aqueous Solutions: Thermodynamics of Copolymer Association. *Macromolecules* **1994**, *27*, 2414–2425.
 - (46) Wanka, G.; Hoffmann, H.; Ulbricht, W. Phase Diagrams and Aggregation Behavior of Poly(oxyethylene)-Poly(oxypropylene)-Poly(oxyethylene) Triblock Copolymers in Aqueous Solutions. *Macromolecules* **1994**, *27*, 4145–4159.
 - (47) López-Barrón, C. R.; Li, D.; Wagner, N. J.; Caplan, J. L. Triblock Copolymer Self-Assembly in Ionic Liquids: Effect of PEO Block Length on the Self-Assembly of PEO-PPO-PEO in Ethylammonium Nitrate. *Macromolecules* **2014**, *47*, 7484–7495.
 - (48) Kabanov, A. V.; Nazarova, I. R.; Astafieva, I. V.; Batrakova, E. V.; Alakhov, V. Y.; Yaroslavov, A. A.; Kabanov, V. A. Micelle Formation and Solubilization of Fluorescent-Probes in Poly(Oxyethylene-B-Oxypropylene-B-Oxyethylene) Solutions. *Macromolecules* **1995**, *28*, 2303–2314.
 - (49) Zhang, S.; Li, N.; Zheng, L.; Li, X.; Gao, Y.; Yu, L. Aggregation Behavior of Pluronic Triblock Copolymer in 1-Butyl-3-Methylimidazolium Type Ionic Liquids. *J. Phys. Chem. B* **2008**, *112*, 10228–10233.
 - (50) Chen, Z.; Greaves, T. L.; Caruso, R. A.; Drummond, C. J. Amphiphile Micelle Structures in the Protic Ionic Liquid Ethylammonium Nitrate and Water. *J. Phys. Chem. B* **2015**, *119*, 179–191.
 - (51) Sharma, S. C.; Atkin, R.; Warr, G. G. The Effect of Ionic Liquid Hydrophobicity and Solvent Miscibility on Pluronic Amphiphile Self-Assembly. *J. Phys. Chem. B* **2013**, *117*, 14568–14575.
 - (52) Atkin, R.; De Fina, L.-M.; Kiederling, U.; Warr, G. G. Structure and Self Assembly of Pluronic Amphiphiles in Ethylammonium Nitrate and at the Silica Surface. *J. Phys. Chem. B* **2009**, *113*, 12201–12213.

- (53) Mortensen, K. Structural Study on the Micelle Formation of PEO-PPO-PEO Triblock Copolymer in Aqueous Solutions. *Macromolecules* **1993**, *26*, 805–812.
- (54) Brown, W.; Schilliin, K.; Hvidt, S. Tribiock Copolymers in Aqueous Solution Studied by Static and Dynamic Light Scatterhg and Oscillatory Shear Measurements. Influence of Relative Block Sizes. *J. Phys. Chem.* **1992**, *9662*, 6038–6044.
- (55) Chen, Z.; Fitzgerald, P. A.; Kobayashi, Y.; Ueno, K.; Watanabe, M.; Warr, G. G.; Atkin, R. Micelle Structure of Novel Diblock Polyethers in Water and Two Protic Ionic Liquids (EAN and PAN). *Macromolecules* **2015**, *48*, 1843–1851.
- (56) Wilhelm, M.; Zhao, C. L.; Wang, Y. C.; Xu, R. L.; Winnik, M. A.; Mura, J. L.; Riess, G.; Croucher, M. D. Polymer Micelle Formation .3. Poly(Styrene-Ethylene Oxide) Block Copolymer Micelle Formation in Water - a Fluorescence Probe Study. *Macromolecules* **1991**, *24*, 1033–1040.
- (57) Villari, V.; Triolo, A.; Micali, N. Evidence of Repulsive Yukawa Tail for Copolymer Micelles in Room Temperature Ionic Liquid. *Soft Matter* **2010**, *6*, 1793.
- (58) Zheng, Y.; Won, Y.-Y.; Bates, F. S.; Davis, H. T.; Scriven, L. E.; Talmon, Y. Directly Resolved Core-Corona Structure of Block Copolymer Micelles by Cryo-Transmission Electron Microscopy. *J. Phys. Chem. B* **1999**, *103*, 10331–10334.
- (59) Won, Y. Y.; Brannan, A. K.; Davis, H. T.; Bates, F. S. Cryogenic Transmission Electron Microscopy (Cryo-TEM) of Micelles and Vesicles Formed in Water by Poly(ethylene Oxide)-Based Block Copolymers. *J. Phys. Chem. B* **2002**, *106*, 3354–3364.
- (60) He, Y.; Li, Z.; Simone, P.; Lodge, T. Self-Assembly of Block Copolymer Micelles in an Ionic Liquid. *J. Am. Chem. Soc.* **2006**, *128*, 2745–2750.
- (61) Bai, Z.; He, Y.; Lodge, T. P. Block Copolymer Micelle Shuttles with Tunable Transfer Temperatures between Ionic Liquids and Aqueous Solutions. *Langmuir* **2008**, *24*, 5284–5290.
- (62) Lee, H. N.; Lodge, T. P. Poly(n -Butyl Methacrylate) in Ionic Liquids with Tunable Lower Critical Solution Temperatures (LCST). *J. Phys. Chem. B* **2011**, *115*, 1971–1977.
- (63) Tamura, S.; Ueki, T.; Ueno, K.; Kodama, K.; Watanabe, M. Thermosensitive Self-Assembly of Diblock Copolymers with Lower Critical Micellization Temperatures in an Ionic Liquid. *Macromolecules* **2009**, *42*, 6239–6244.
- (64) Ueki, T.; Nakamura, Y.; Lodge, T. P.; Watanabe, M. Light-Controlled Reversible Micellization of a Diblock Copolymer in an Ionic Liquid. *Macromolecules* **2012**, *45*, 7566–7573.
- (65) Lee, H. N.; Bai, Z.; Newell, N.; Lodge, T. P. Micelle/inverse Micelle Self-Assembly of a PEO-PNIPAm Block Copolymer in Ionic Liquids with Double Thermoresponse. *Macromolecules* **2010**, *43*, 9522–9528.
- (66) Zheng, L.; Chai, Y.; Liu, Y.; Zhang, P. Controlled RAFT Synthesis of Polystyrene-B-Poly(acrylic Acid)-B-Polystyrene Block Copolymers and Their Self-Assembly in an Ionic Liquid [BMIM][PF6]. *E-Polymers* **2011**, *11*, 436–443.
- (67) DeRita, L. Self-Assembly of Pluornic Polymer Systems in Ionic Liquids. Undergraduate Dissertation, Univeristy of Delaware, Newark, DE, 2013.
- (68) López-Barrón, C. R.; Chen, R.; Wagner, N. J.; Beltramo, P. J. Self-Assembly of Pluronic F127 Diacrylate in Ethylammonium Nitrate: Structure, Rheology, and Ionic Conductivity before and after Photo-Cross-Linking. *Macromolecules* **2016**, *49*, 5179–5189.
- (69) Laflèche, F.; Taco, N.; Dominique, D.; Yves, G.; Taton, D. Association of Adhesive Spheres Formed by Hydrophobically End-Capped PEO. 2. Influence of the Alkyl End-Group Length and the Chain Backbone Architecture. *Macromolecules* **2003**, *36*, 1341–1348.
- (70) Anderson, J. a; Lorenz, C. D.; Travasset, a. Micellar Crystals in Solution from Molecular Dynamics Simulations. *J. Chem. Phys.* **2008**, *128*, 184906.
- (71) Meli, L.; Lodge, T. P. Equilibrium vs Metastability: High-Temperature Annealing of Spherical Block Copolymer Micelles in an Ionic Liquid. *Macromolecules* **2009**, *42*, 580–583.
- (72) Meli, L.; Santiago, J. M.; Lodge, T. P. Path-Dependent Morphology and Relaxation Kinetics of Highly Amphiphilic Diblock Copolymer Micelles in Ionic Liquids. *Macromolecules* **2010**, *43*, 2018–2027.

- (73) Ueki, T.; Watanabe, M. Upper Critical Solution Temperature Behavior of Poly(N-Isopropylacrylamide) in an Ionic Liquid and Preparation of Thermo-Sensitive Nonvolatile Gels. *Chem. Lett.* **2006**, *35*, 964–965.
- (74) Kodama, K.; Nanashima, H.; Ueki, T.; Kokubo, H.; Watanabe, M. Lower Critical Solution Temperature Phase Behavior of Linear Polymers in Imidazolium-Based Ionic Liquids: Effects of Structural Modifications. *Langmuir* **2009**, *25*, 3820–3824.
- (75) Ueki, T.; Watanabe, M. Lower Critical Solution Temperature Behavior of Linear Polymers in Ionic Liquids and the Corresponding Volume Phase Transition of Polymer Gels. *Langmuir* **2007**, *23*, 988–990.
- (76) Tsuda, R.; Kodama, K.; Ueki, T.; Kokubo, H.; Imabayashi, S.; Watanabe, M. LCST-Type Liquid-Liquid Phase Separation Behaviour of Poly(ethylene Oxide). *Chem. Commun.* **2008**, No. 40, 4939–4941.
- (77) Lee, H. N.; Lodge, T. P. Lower Critical Solution Temperature (LCST) Phase Behavior of Poly(ethylene Oxide) in Ionic Liquids. *J. Phys. Chem. Lett.* **2010**, *1*, 1962–1966.
- (78) Lee, H. N.; Newell, N.; Bai, Z.; Lodge, T. P. Unusual Lower Critical Solution Temperature Phase Behavior of Poly(ethylene Oxide) in Ionic Liquids. *Macromolecules* **2012**, *45*, 3627–3633.
- (79) Ueki, T.; Watanabe, M.; Lodge, T. P. Doubly Thermosensitive Self-Assembly of Diblock Copolymers in Ionic Liquids. *Macromolecules* **2009**, *42*, 1315–1320.
- (80) He, Y.; Boswell, P. G.; Bühlmann, P.; Lodge, T. P. Ion Gels by Self-Assembly of a Triblock Copolymer in an Ionic Liquid. *J. Phys. Chem. B* **2007**, *111*, 4645–4652.
- (81) Zhang, S.; Lee, K. H.; Sun, J.; Frisbie, C. D.; Lodge, T. P. Viscoelastic Properties, Ionic Conductivity, and Materials Design Considerations for Poly(styrene-B-Ethylene Oxide-B-Styrene)-Based Ion Gel Electrolytes. *Macromolecules* **2011**, *44*, 8981–8989.
- (82) Zhang, S.; Lee, K. H.; Frisbie, C. D.; Lodge, T. P. Ionic Conductivity, Capacitance, and Viscoelastic Properties of Block Copolymer-Based Ion Gels. *Macromolecules* **2011**, *44*, 940–949.
- (83) He, Y.; Lodge, T. P. A Thermoreversible Ion Gel by Triblock Copolymer Self-Assembly in an Ionic Liquid. *Chem. Commun.* **2007**, *16*, 2732–2734.
- (84) Virgili, J. M. Studies of Block Copolymer Thin Films and Mixtures with an Ionic Liquid. Ph.D. Dissertation, University of California, Berkeley, CA, 2009.
- (85) He, Y.; Lodge, T. P. The Micellar Shuttle: Thermoreversible, Intact Transfer of Block Copolymer Micelles between an Ionic Liquid and Water. *J. Am. Chem. Soc.* **2006**, *128*, 12666–12667.
- (86) Meier, W. Polymer Nanocapsules. *Chem. Soc. Rev.* **2000**, *29*, 295–303.
- (87) Cooper, A.; Londono, J.; Wignall, G.; McClain, J.; Samulski, E.; Lin, J.; Dobrynin, A.; Rubinstein, M.; Burke, A.; Frechet, J.; DeSimone, J. Extraction of a Hydrophilic Compound from Water into Liquid CO₂ Using Dendritic Surfactants. *Nature* **1997**, *389*, 368–371.
- (88) Sunder, A.; Krämer, M.; Hanselmann, R.; Mülhaupt, R.; Frey, H. Molecular Nanocapsules Based on Amphiphilic Hyperbranched Polyglycerols. *Angew. Chem. Int. Ed.* **1999**, *38*, 3552–3555.
- (89) Chechik, V.; Zhao, M.; Crooks, R. M. Self-Assembled Inverted Micelles Prepared from a Dendrimer Template: Phase Transfer of Encapsulated Guests. *J. Am. Chem. Soc.* **1999**, 4910–4911.
- (90) Vriezema, D. M.; Aragonès, M. C.; Elemans, J. A. A. W.; Cornelissen, J. J. L. M.; Rowan, A. E.; Nolte, R. J. M. Self-Assembled Nanoreactors. *Chem. Rev.* **2005**, 1445–1489.
- (91) Dwar, T.; Paetzold, E.; Oehme, G. Reactions in Micellar Systems. *Angew. Chem. Int. Ed.* **2005**, *44*, 7174–7199.
- (92) Bai, Z.; He, Y.; Young, N. P.; Lodge, T. P. A Thermoreversible Micellization-Transfer-Demicellization Shuttle between Water and an Ionic Liquid. *Macromolecules* **2008**, *41*, 6615–6617.
- (93) Guerrero-Sanchez, C.; Wouters, D.; Hoepfener, S.; Hoogenboom, R.; Schubert, U. S. Micellar Dye Shuttle between Water and an Ionic Liquid. *Soft Matter* **2011**, *7*, 3827–3831.
- (94) Bai, Z.; Lodge, T. P. Pluronic Micelle Shuttle between Water and an Ionic Liquid. *Langmuir* **2010**, *26*, 8887–8892.

- (95) Saeki, S.; Kuwahara, N.; Nakata, M.; Kaneko, M. Upper and Lower Critical Solution Temperatures in Poly (Ethylene Glycol) Solutions. *Polymer*. **1976**, *17*, 685–689.
- (96) Bai, Z.; Lodge, T. P. Polymersomes with Ionic Liquid Interiors Dispersed in Water. *J. Am. Chem. Soc.* **2010**, *132*, 16265–16270.
- (97) Bai, Z.; Zhao, B.; Lodge, T. P. Bilayer Membrane Permeability of Ionic Liquid-Filled Block Copolymer Vesicles in Aqueous Solution. *J. Phys. Chem. B* **2012**, *116*, 8282–8289.
- (98) Bai; Lodge. Thermodynamics and Mechanism of the Block Copolymer Micelle Shuttle between Water and an Ionic Liquid. *J. Phys. Chem. B* **2009**, *113*, 14151–14157.
- (99) Hoarfrost, M. L. Ion Transport in Nanostructured Block Copolymer/Ionic Liquid Membranes. Ph.D. Dissertation, University of California, Berkeley, Berkeley, CA, 2012.
- (100) Lai, C.; Russel, W. B.; Register, R. A. Scaling of Domain Spacing in Concentrated Solutions of Block Copolymers in Selective Solvents. *Macromolecules* **2002**, *35*, 4044–4049.
- (101) Hanley, K. J.; Lodge, T. P.; Huang, C. I. Phase Behavior of a Block Copolymer in Solvents of Varying Selectivity. *Macromolecules* **2000**, *33*, 5918–5931.
- (102) Simone, P. M.; Lodge, T. P. Phase Behavior and Ionic Conductivity of Concentrated Solutions of Polystyrene-Poly(ethylene Oxide) Diblock Copolymers in an Ionic Liquid. *ACS Appl. Mater. Interfaces* **2009**, *1*, 2812–2820.
- (103) Park, J. W.; Kim, H.; Han, M. Polymeric Self-Assembled Monolayers Derived from Surface-Active Copolymers: A Modular Approach to Functionalized Surfaces. *Chem. Soc. Rev.* **2010**, *39*, 2935–2947.
- (104) Simone, P. M.; Lodge, T. P. Lyotropic Phase Behavior of Polybutadiene-Poly (Ethylene Oxide) Diblock Copolymers in Ionic Liquids. *Macromolecules* **2008**, *41*, 1753–1759.
- (105) Virgili, J. M.; Hexemer, A.; Pople, J. A.; Balsara, N. P.; Segalman, R. A. Phase Behavior of Polystyrene-Block-poly(2-Vinylpyridine) Copolymers in a Selective Ionic Liquid Solvent. *Macromolecules* **2009**, *42*, 4604–4613.
- (106) Virgili, J. M.; Hoarfrost, M. L.; Segalman, R. A. Effect of an Ionic Liquid Solvent on the Phase Behavior of Block Copolymers. *Macromolecules* **2010**, *43*, 5417–5423.
- (107) Miranda, D. F.; Russell, T. P.; Watkins, J. J. Ordering in Mixtures of a Triblock Copolymer with a Room Temperature Ionic Liquid. *Macromolecules* **2010**, *43*, 10528–10535.
- (108) Wang, L.; Chen, X.; Chai, Y.; Hao, J.; Sui, Z.; Zhuang, W.; Sun, Z. Lyotropic Liquid Crystalline Phases Formed in an Ionic Liquid. *Chem. Commun.* **2004**, *6*, 2840–2841.
- (109) Zhang, G.; Chen, X.; Zhao, Y.; Ma, F.; Jing, B.; Qiu, H. Lyotropic Liquid-Crystalline Phases Formed by Pluronic P123 in Ethylammonium Nitrate. *J. Phys. Chem. B* **2008**, *112*, 6578–6584.
- (110) McConnell, G. A.; Gast, A. P.; Huang, J. S.; Smith, S. D. Disorder-Order Transitions in Soft Sphere Polymer Micelles. *Phys. Rev. Lett.* **1993**, *71*, 2102–2105.
- (111) Mortensen, K.; Batsberg, W.; Hvidt, S. Effects of PEO - PPO Diblock Impurities on the Cubic Structure of Aqueous PEO - PPO - PEO Pluronics Micelles : Fcc and Bcc Ordered Structures in F127. *Macromolecules* **2008**, *41*, 1720–1727.
- (112) Chen, R.; López-Barrón, C. R.; Wagner, N. J. Co-Micellization of Binary Mixture of PEO-PPO-PEO Tri-Block Copolymer P123 and F127 in Ethylammonium Nitrate. *In prepara.*
- (113) Chen, R.; López-Barrón, C. R.; Wagner, N. J. Tunable Rheology, Microstructure and Shear Alignment of Thermo-Reversible Soft Micellar Crystals in Ionic Liquid. *In prepara.*
- (114) Mortensen, K.; Brown, W.; Nordén, B. Inverse Melting Transition and Evidence of Three-Dimensional Cubatic Structure in a Block-Copolymer Micellar System. *Phys. Rev. Lett.* **1992**, *68*, 2340–2343.
- (115) Walker, L. M. Rheology and Structure of Worm-like Micelles. *Curr. Opin. Colloid Interface Sci.* **2001**, *6*, 451–456.
- (116) Eberle, A. P. R.; Porcar, L. Flow-SANS and Rheo-SANS Applied to Soft Matter. *Curr. Opin. Colloid Interface Sci.* **2012**, *17*, 33–43.
- (117) Phoon, C. L.; Higgins, J. S.; Allegra, G.; Leeuwen, P. V.; Staples, E. Shear Induced Crystallization and Melting of a Micellar Solution. *Proc. R. Soc. A Math. Phys. Eng. Sci.* **1993**, *442*, 221–230.

- (118) McConnell, G. A.; Lin, M. Y.; Gast, A. P. Long-Range Order in Polymeric Micelles Under Steady Shear. *Macromolecules* **1995**, *28*, 6754–6764.
- (119) Berret, J. F.; Molino, F.; Porte, G.; Diat, O.; Lindner, P. The Shear-Induced Transition between Oriented Textures and Layer-Sliding-Mediated Flows in a Micellar Cubic Crystal. *J. Phys. Condens. Matter* **1996**, *8*, 9513–9517.
- (120) Slawecki, T.; Glinka, C.; Hammouda, B. Shear-Induced Micellar Crystal Structures in an Aqueous Triblock Copolymer Solution. *Phys. Rev. E* **1998**, *58*, R4084–R4087.
- (121) Jiang, J.; Burger, C.; Li, C.; Li, J.; Lin, M. Y.; Colby, R. H.; Rafailovich, M. H.; Sokolov, J. C. Shear-Induced Layered Structure of Polymeric Micelles by SANS. *Macromolecules* **2007**, *40*, 4016–4022.
- (122) Jiang, J.; Malal, R.; Li, C.; Lin, M. Y.; Colby, R. H.; Gersappe, D.; Rafailovich, M. H.; Sokolov, J. C.; Cohn, D. Rheology of Thermoreversible Hydrogels from Multiblock Associating Copolymers. *Macromolecules* **2008**, *41*, 3646–3652.
- (123) Ackerson, B. J.; Pusey, P. N. Shear-Induced Order in Suspensions of Hard Spheres. *Phys. Rev. Lett.* **1988**, *61*, 1033–1036.
- (124) Chen, L. B.; Zukoski, C. F.; Ackerson, B. J.; Hanley, H. J. M.; Straty, G. C.; Barker, J.; Glinka, C. J. Structural-Changes and Orientational Order in a Sheared Colloidal Suspension. *Phys. Rev. Lett.* **1992**, *69*, 688–691.
- (125) Wu, Y. L.; Derks, D.; van Blaaderen, A.; Imhof, A. Melting and Crystallization of Colloidal Hard-Sphere Suspensions under Shear. *Proc. Natl. Acad. Sci. U. S. A.* **2009**, *106*, 10564–10569.
- (126) López-Barrón, C. R.; Wagner, N. J.; Porcar, L. Layering, Melting, and Recrystallization of a Close-Packed Micellar Crystal under Steady and Large-Amplitude Oscillatory Shear Flows. *J. Rheol.* **2015**, *59*, 793–820.
- (127) Porcar, L.; Pozzo, D.; Langenbacher, G.; Moyer, J.; Butler, P. D. Rheo-Small-Angle Neutron Scattering at the National Institute of Standards and Technology Center for Neutron Research. *Rev. Sci. Instrum.* **2011**, *82*, 83902.
- (128) Gurnon, A. K.; Godfrin, P. D.; Wagner, N. J.; Eberle, A. P. R.; Butler, P.; Porcar, L. Measuring Material Microstructure under Flow Using 1-2 Plane Flow-Small Angle Neutron Scattering. *J. Vis. Exp.* **2014**, *84*, e51068.
- (129) López-Barrón, C. R.; Porcar, L.; Eberle, A. P. R.; Wagner, N. J. Dynamics of Melting and Recrystallization in a Polymeric Micellar Crystal Subjected to Large Amplitude Oscillatory Shear Flow. *Phys. Rev. Lett.* **2012**, *108*, 258301.
- (130) Dreiss, C. A. Wormlike Micelles: Where Do We Stand? Recent Developments, Linear Rheology and Scattering Techniques. *Soft Matter* **2007**, *3*, 956.
- (131) Cates, M. E.; Fielding, S. M. *Rheology of Giant Micelles*. Taylor & Francis 2007.
- (132) Zana, R.; Kaler, E. W. *Giant Micelles: Properties and Applications*; CRC Press: Boca Raton, 2007.
- (133) Berret, J. F. Rheology of Wormlike Micelles: Equilibrium Properties and Shear Banding Transitions. In *Molecular Gels: Materials with Self-Assembled Fibrillar Networks*; Springer Netherlands: Dordrecht, 2006; pp 667–720.
- (134) Castelletto, V.; Parras, P.; Hamley, I. W.; Bäverbäck, P.; Pedersen, J. S.; Panine, P. Wormlike Micelle Formation and Flow Alignment of a Pluronic Block Copolymer in Aqueous Solution. *Langmuir* **2007**, *23*, 6896–6902.
- (135) Holmqvist, P.; Alexandridis, P.; Lindman, B. Modification of the Microstructure in Block Copolymer–Water–“Oil” Systems by Varying the Copolymer Composition and the “Oil” Type: Small-Angle X-Ray Scattering and Deuterium-NMR Investigation. *J. Phys. Chem. B* **1998**, *102*, 1149–1158.
- (136) Miranda, D. F.; Versek, C.; Tuominen, M. T.; Russell, T. P.; Watkins, J. J. Cross-Linked Block Copolymer/ionic Liquid Self-Assembled Blends for Polymer Gel Electrolytes with High Ionic Conductivity and Mechanical Strength. *Macromolecules* **2013**, *46*, 9313–9323.
- (137) Sutto, T. E. Hydrophobic and Hydrophilic Interactions of Ionic Liquids and Polymers in Solid

- Polymer Gel Electrolytes. *J. Electrochem. Soc.* **2007**, *154*, P101-P107.
- (138) Lewandowski, A.; Świdarska, A. New Composite Solid Electrolytes Based on a Polymer and Ionic Liquids. *Solid State Ionics* **2004**, *169*, 21–24.
- (139) Zhu, C.; Cheng, H.; Yang, Y. Electrochemical Characterization of Two Types of PEO-Based Polymer Electrolytes with Room-Temperature Ionic Liquids. *J. Electrochem. Soc.* **2008**, *155*, A569-A575.
- (140) Kim, Y. H.; Cheruvally, G.; Choi, J. W.; Ahn, J. H.; Kim, K. W.; Ahn, H. J.; Choi, D. S.; Song, C. E. Electrochemical Properties of PEO-Based Polymer Electrolytes Blended with Different Room Temperature Ionic Liquids. *Macromol. Symp.* **2007**, 249-250, 183-189.
- (141) Fuller, J.; Breda, A. C.; Carlin, R. T. Ionic Liquid-Polymer Gel Electrolytes. *J. Electrochem. Soc.* **1997**, *144*, L67–L70.
- (142) Singh, B.; Sekhon, S. S. Ion Conducting Behaviour of Polymer Electrolytes Containing Ionic Liquids. *Chem. Phys. Lett.* **2005**, *414*, 34–39.
- (143) Yeon, S. H.; Kim, K. S.; Choi, S.; Cha, J. H.; Lee, H. Characterization of PVdF(HFP) Gel Electrolytes Based on 1-(2-Hydroxyethyl)-3-Methyl Imidazolium Ionic Liquids. *J. Phys. Chem. B* **2005**, *109*, 17928–17935.
- (144) Scott, M. P.; Brazel, C. S.; Benton, M. G.; Mays, J. W.; Holbrey, J. D.; Rogers, R. D. Application of Ionic Liquids as Plasticizers for Poly(methyl Methacrylate). *Chem. Commun.* **2002**, *3*, 1370–1371.
- (145) Susan, M. A. B. H.; Kaneko, T.; Noda, A.; Watanabe, M. Ion Gels Prepared by in Situ Radical Polymerization of Vinyl Monomers in an Ionic Liquid and Their Characterization as Polymer Electrolytes. *J. Am. Chem. Soc.* **2005**, *127*, 4976–4983.
- (146) Seki, S.; Susan, M. A. B. H.; Kaneko, T.; Tokuda, H.; Noda, A.; Watanabe, M. Distinct Difference in Ionic Transport Behavior in Polymer Electrolytes Depending on the Matrix Polymers and Incorporated Salts. *J. Phys. Chem. B* **2005**, *109*, 3886–3892.
- (147) Jana, S.; Parthiban, A.; Chai, C. L. L. Transparent, Flexible and Highly Conductive Ion Gels from Ionic Liquid Compatible Cyclic Carbonate Network. *Chem. Commun.* **2010**, *46*, 1488–1490.
- (148) Klingshirn, M. A.; Spear, S. K.; Subramanian, R.; Holbrey, J. D.; Huddleston, J. G.; Rogers, R. D. Gelation of Ionic Liquids Using a Cross-Linked Poly(ethylene Glycol) Gel Matrix. *Chem. Mater.* **2004**, *16*, 3091–3097.
- (149) Néouze, M. A.; Le Bideau, J.; Gaveau, P.; Bellayer, S.; Vioux, A. Ionogels, New Materials Arising from the Confinement of Ionic Liquids within Silica-Derived Networks. *Chem. Mater.* **2006**, *18*, 3931–3936.
- (150) Matsumoto, K.; Endo, T. Confinement of Ionic Liquid by Networked Polymers Based on Multifunctional Epoxy Resins. *Macromolecules* **2008**, *41*, 6981–6986.
- (151) Matsumoto, K.; Endo, T. Synthesis of Ion Conductive Networked Polymers Based on an Ionic Liquid Epoxide Having a Quaternary Ammonium Salt Structure. *Macromolecules* **2009**, *42*, 4580–4584.
- (152) Gu, Y.; Zhang, S.; Martinetti, L.; Lee, K. H.; McIntosh, L. D.; Frisbie, C. D.; Lodge, T. P. High Toughness, High Conductivity Ion Gels by Sequential Triblock Copolymer Self-Assembly and Chemical Cross-Linking. *J. Am. Chem. Soc.* **2013**, *135*, 9652–9655.
- (153) López-Barrón, C. R.; Chen, R.; Wagner, N. J. Ultrastretchable Iono-Elastomers with Mechanoelectrical Response. *ACS Macro Lett.* **2016**, *5*, 1332–1338.
- (154) Rogers, J. A.; Someya, T.; Huang, Y. Materials and Mechanics for Stretchable Electronics. *Science*. **2010**, *327*, 1603–1607.
- (155) Seki, S.; Kobayashi, Y.; Miyashiro, H.; Ohno, Y.; Usami, A.; Mita, Y.; Kihira, N.; Watanabe, M.; Terada, N. Lithium Secondary Batteries Using Modified-Imidazolium Room-Temperature Ionic Liquid. *J. Phys. Chem. B* **2006**, *110*, 10228–10230.
- (156) Zakeeruddin, S. M.; Grätzel, M. Solvent-Free Ionic Liquid Electrolytes for Mesoscopic Dye-Sensitized Solar Cells. *Adv. Funct. Mater.* **2009**, *19*, 2187–2202.
- (157) Lu, W.; Fadeev, A. G.; Qi, B.; Smela, E.; Mattes, B. R.; Ding, J.; Spinks, G. M.; Mazurkiewicz, J.;

- Zhou, D.; Wallace, G. G.; MacFarlane, D. R.; Forsyth, S. A.; Forsyth, M. Use of Ionic Liquids for Pi-Conjugated Polymer Electrochemical Devices. *Science*. **2002**, *297*, 983–987.
- (158) Ding, J.; Zhou, D.; Spinks, G.; Wallace, G.; Forsyth, S.; Forsyth, M.; MacFarlane, D. Use of Ionic Liquids as Electrolytes in Electromechanical Actuator Systems Based on Inherently Conducting Polymers. *Chem. Mater.* **2003**, *15*, 2392–2398.
- (159) Cho, J. H.; Lee, J.; Xia, Y.; Kim, B.; He, Y.; Renn, M. J.; Lodge, T. P.; Frisbie, C. D. Printable Ion-Gel Gate Dielectrics for Low-Voltage Polymer Thin-Film Transistors on Plastic. *Nat. Mater.* **2008**, *7*, 900–906.
- (160) Cho, J. H.; Lee, J.; He, Y.; Kim, B.; Lodge, T. P.; Frisbie, C. D. High-Capacitance Ion Gel Gate Dielectrics with Faster Polarization Response Times for Organic Thin Film Transistors. *Adv. Mater.* **2008**, *20*, 686–690.
- (161) Zhang, L.; Eisenberg, A. Multiple Morphologies of “Crew-Cut” Aggregates of Polystyrene-B-Poly(acrylic Acid) Block Copolymers. *Science*. **1995**, *268*, 1728–1731.
- (162) Creutz, S.; van Stam, J.; De Schryver, F. C.; Jérôme, R. Dynamics of Poly((dimethylamino)alkyl Methacrylate-Block-Sodium Methacrylate) Micelles. Influence of Hydrophobicity and Molecular Architecture on the Exchange Rate of Copolymer Molecules. *Macromolecules* **1998**, *31*, 681–689.
- (163) Loppinet, B.; Sigel, R.; Larsen, A.; Fytas, G.; Vlassopoulos, D.; Liu, G. Structure and Dynamics in Dense Suspensions of Micellar Nanocolloids. *Langmuir* **2000**, *16*, 6480–6484.
- (164) Discher, B. M.; Won, Y. Y.; Ege, D. S.; Lee, J. C. M.; Bates, F. S.; Discher, D. E.; Hammer, D. A. Polymersomes: Tough Vesicles Made from Diblock Copolymers. *Science*. **1999**, *284*, 1143–1146.
- (165) O’Reilly, R. K.; Joralemon, M. J.; Wooley, K. L.; Hawker, C. J. Functionalization of Micelles and Shell Cross-Linked Nanoparticles Using Click Chemistry. *Chem. Mater.* **2005**, *17*, 5976–5988.
- (166) Joralemon, M. J.; O’Reilly, R. K.; Hawker, C. J.; Wooley, K. L. Shell Click-Crosslinked (SCC) Nanoparticles: A New Methodology for Synthesis and Orthogonal Functionalization. *J. Am. Chem. Soc.* **2005**, *127*, 16892–16899.
- (167) Blach, D.; Pességo, M.; Silber, J. J.; Correa, N. M.; García-Río, L.; Falcone, R. D. Ionic Liquids Entrapped in Reverse Micelles as Nanoreactors for Bimolecular Nucleophilic Substitution Reaction. Effect of the Confinement on the Chloride Ion Availability. *Langmuir* **2014**, *30*, 12130–12137.
- (168) Marrucho, I. M.; Branco, L. C.; Rebelo, L. P. N. Ionic Liquids in Pharmaceutical Applications. *Annu. Rev. Chem. Biomol. Eng.* **2014**, *5*, 527–546.
- (169) Xu, S.; Zhang, Y.; Cho, J.; Lee, J.; Huang, X.; Jia, L.; Fan, J. A.; Su, Y.; Su, J.; Zhang, H.; Cheng, H.; Lu, B.; Yu, C.; Chuang, C.; Kim, T. I.; Song, T.; Shigeta, K.; Kang, S.; Dagdeviren, C.; Petrov, I.; Braun, P. V.; Huang, Y.; Paik, U.; Rogers, J. A. Stretchable Batteries with Self-Similar Serpentine Interconnects and Integrated Wireless Recharging Systems. *Nat. Commun.* **2013**, *4*, 1543.
- (170) Kaltenbrunner, M.; Sekitani, T.; Reeder, J.; Yokota, T.; Kuribara, K.; Tokuhara, T.; Drack, M.; Schwödiauer, R.; Graz, I.; Bauer-Gogonea, S.; Bauer, S.; Someya, T. An Ultra-Lightweight Design for Imperceptible Plastic Electronics. *Nature* **2013**, *499*, 458–463.
- (171) Sekitani, T.; Noguchi, Y.; Hata, K.; Fukushima, T.; Aida, T.; Someya, T. A Rubberlike Stretchable Active Matrix Using Elastic Conductors. *Science*. **2008**, *321*, 1468–1472.
- (172) Kim, D. H.; Ahn, J. H.; Choi, W. M.; Kim, H.-S.; Kim, T. H.; Song, J.; Huang, Y. Y.; Liu, Z.; Lu, C.; Rogers, J. A. Stretchable and Foldable Silicon Integrated Circuits. *Science*. **2008**, *320*, 507–511.
- (173) Stoppa, M.; Chiolerio, A. Wearable Electronics and Smart Textiles: A Critical Review. *Sensors* **2014**, *14*, 11957–11992.
- (174) Appetecchi, G. B.; Zane, D.; Scrosati, B. PEO-Based Electrolyte Membranes Based on LiBC4O8 Salt. *J. Electrochem. Soc.* **2004**, *151*, A1369.
- (175) Richards, J. J.; Gagnon, C. V. L.; Krzywon, J. R.; Wagner, N. J.; Butler, P. D. Dielectric RheoSANS –Simultaneous Interrogation of Impedance, Rheology and Small Angle Neutron Scattering of Complex Fluids. *J. Vis. Exp.* e55318 doi:10.3791/55318